International Journal of Heat and Mass Transfer 64 (2013) 591 -608

Flow boiling heat transfer of HFO1234yf and HFC32 refrigerant mixtures in a smooth horizontal tube: Part II. Prediction method

Minxia Li[a], Chaobin Dang[b*], Eiji Hihara[b]

[a] Key Laboratory of Medium-Low Temperature Energy Efficient Utilization, Ministry of Education, Department of Thermal Engineering, Tianjin University, Tianjin, China

[b] Institute of Environmental Studies, Graduate School of Frontier Sciences, The University of Tokyo, 5-1-5 Kashiwanoha, Kashiwa-shi, Chiba, Japan

Abstract: A prediction model has been developed using the results of prior experimental investigations into the flow boiling heat transfer of pure HFO1234yf, HFC32, and their refrigerant mixtures at two mass fractions (80/20 and 50/50 by mass%) in a smooth horizontal tube having an inner diameter of 2 mm. In the prior experiment, the saturation temperature was 15 °C, the mass fluxes ranged from 100 to 400 kg/m^{2}s, and the heat fluxes ranged from 6 to 24 kW/m^2. In this paper, we propose a new semi-empirical correlation for pure refrigerants based on the superposition of the contributions from nucleate boiling and convection. We introduced two new factors in the correlation to account for the effects of the convection on two-phase flow and nucleate boiling. Comparisons between the experimental results and the predictions of seven correlations showed that the proposed correlation had reasonable agreement with the magnitudes and trends of the variations in the measured heat transfer coefficient of pure HFO1234yf, HFC32, and the 50/50 mass% mixture (with a mean absolute error of approximately 20%) when the average properties of the mixtures were used. However, this simple approach was found to overestimate the experimental results for the 80/20 mass% mixture. The inhomogeneity of the concentration in the mixture significantly affects its heat transfer with a high temperature glide; the predicted deviation was large when only the average properties of the mixture are considered. After taking into consideration the effects of mass diffusion on the flow boiling heat transfer of refrigerant mixtures, we introduced suppression factors for the mixture into both the existing and proposed correlations. Superior prediction accuracies were obtained using these modified correlations. When predicting the heat transfer coefficients of the refrigerant mixtures of HFO1234yf and HFC32 (80/20 and 50/50 by mass%), the average deviation of the proposed correlation with suppression factors was less than 20%.

Keywords: HFO1234yf; HFC32; Refrigerant mixture; Flow boiling heat transfer; Prediction model; low GWP refrigerant

NOMENCLATURE

A	correcting factor
a_c	thermal diffusion factor, m^2/s
Bo	boiling number, $Bo = q/(Gh_{lv})$
c_{pl}	specific heat at constant pressure in liquid phase, J/kgK
C	correcting factor
d,D	inner diameter, m
D_m	mass diffusion factor, m^2/s
F	convective enhancement factor
Fr	Froude number, $Fr = u^2/(gd)$
G	mass flux, kg/m^{2}s
h	boiling heat transfer coefficient, W/m^{2}K
k	Boltzmann's constant
m	mass, mol
m_f	mass flow rate, kg/s
n	particle number density of fluid
p	pressure, Pa
p_{cr}	critical pressure, Pa
p_r	reduced pressure p/p_{cr}

* Corresponding author. dangcb@k.u-tokyo.ac.jp

Pr	Prandtl number, $\mathrm{Pr} = \mu/(\rho\alpha_c)$
q	heat flux, W/m^2
R	diameter of bubble, m
Re	Reynolds number, $\mathrm{Re} = Gd/\mu$
S	suppression factor
T	temperature, K
T_{wall}	inner-wall temperature, K
T_{sat}	fluid saturation temperature, K
We	Weber number, $We = G^2 d/(\rho\sigma)$
x	vapor quality
$\tilde{x}$	mole fraction of volatile component in liquid phase
X, X_{tt}	Lockhart–Martinelli parameter
$\tilde{y}$	mole fraction of volatile component in vapor phase
z	coordinate along tube direction, m
Z	compressibility factor
Δh_v, h_{lv}	latent heat, J/kg
ΔT	superheat, K
ΔT_I	ideal superheat, K
ΔT_{bp}	temperature difference between dew point and bubble point, K
ΔT^E	maximum rise in local bubble point temperature, K

Greek symbols

λ	thermal conductivity, W/mK
μ	viscosity, Pas
ρ	density, kg/m^3
σ	surface tension, N/m
$\tilde{\sigma}_i$	diameter of species i, m
Φ	two-phase flow multiplier
γ	activity coefficient
η	packing fraction
ε	void fraction

Subscripts

b	bubble
b0	liquid feed to a reboiler
bi	vapor leaving a reboiler
bk	bulk
cal	calculated
CS	Carnahan–Starling equation of state
cv	convective boiling
exp	experimental
I, id	ideal
in	interface
int	liquid–vapor interface
kin	kinetic
L, l	liquid phase
l0	all flow as liquid phase
m	mix, mixture
nb	nucleate boiling
P	pressure
PY	Percus–Yevick virial equation
T	temperature
tp	two-phase
v	gas phase, vapor phase
v0	all flow as vapor phase
1	component 1

2 component 2

Superscripts

Ens Enskog transport equation

1 INTRODUCTION

The refrigerants used in refrigeration systems typically have measurable environmental effects including the ozone depletion potential (ODP) and global warming potential (GWP). Today, either hydrofluorocarbons (HFCs) with high GWP values or hydrochlorofluorocarbons (HCFCs) with small ODP values are used in stationary air conditioners. Hence, it is crucial to replace these refrigerants with low GWP variants. HFO1234yf, a newly developed refrigerant with a low GWP of 4, has been proposed as a drop-in solution for current automotive air conditioners [1]. However, HFO1234yf has smaller latent heat than HFC410A. When it is substituted directly into a stationary air conditioner, the coefficient of performance (COP) of the system decreases significantly. The COP might be improved by combining a highly efficient refrigerant, such as HFC32, with a low GWP refrigerant. Hence, a refrigerant mixture of HFO1234yf and HFC32 was considered, and experimental measurements were conducted to clarify its flow boiling heat transfer characteristics. The results were reported in Part I of this paper [2]. The experiments were performed at an evaporation temperature of 15 °C, refrigerant mass flux within a range from 100 to 400 kg/m^{2}s, and heat flux of 6–24 kW/m^2. The heat transfer coefficient of the HFO1234yf + HFC32 refrigerant mixture (80/20 by mass%) was 20%–50% lower than that of pure HFC32 and 10%–30% lower than that of HFO1234yf. When the concentration of HFC32 was increased to 50%, the heat transfer coefficient of the mixture became 10%–20% higher than that of pure HFO1234yf but was still 20%–40% lower than that of HFC32.

In this paper, the experimental heat transfer coefficients determined in Part I are compared with the predicted results obtained using some prediction models from the literature. Further, a new correlation is proposed to predict the heat transfer coefficients of pure HFC32, HFO1234yf, and two HFO1234yf + HFC32 mixtures (80/20 and 50/50 by mass%). Because the mechanisms of flow boiling heat transfer in the pre-dryout region are different from those in the post-dryout region, the prediction of heat transfer coefficients described in this paper focuses mainly on the pre-dryout region.

2 SURVEY OF LITERATURE ON FLOW BOILING HEAT TRANSFER

For the flow boiling of pure refrigerants, the most widely accepted heat transfer model is that of Chen's correlation [3], in which the heat transfer coefficient of a two-phase flow, h_{tp}, is a linear superposition of the coefficients of nucleate boiling (h_{nb}) and convective heat transfer (h_{cv}).

$$h_{tp} = \left(Sh_{nb} + Fh_{cv} \right) \tag{1}$$

In Chen's original correlation, h_{nb} and h_{cv} were calculated using the correlation proposed by Forster and Zuber [4] and the Dittus–Boelter equation, respectively. Chen also defined a suppression factor S as a function of the Reynolds number to account for the suppression of the nucleate boiling heat transfer by the effects of convection. The factor F, which is defined to account for the ratio of the two-phase Reynolds number to the liquid-phase Reynolds number, was introduced to revise h_{cv}. Subsequently, Chen and Tuzla [5] experimentally investigated the contributions of convection and boiling to saturated convective flow boiling. Their results indicate that, in comparison with single-phase flow, two-phase flow enhances the convection heat transfer and suppresses the nucleate boiling heat transfer. Many researchers have adopted the superposition formula proposed by Chen, after modifications to the factors F and S in accordance with their own experimental results.

For example, the Gungor–Winterton correlation [6], given by Eq. (2), is a modification of the Chen correlation:

$$h_{tp} = \left(Sh_{nb} + Eh_{cv} \right) \tag{2}$$

where E is an enhancement factor for the convection defined by Gungor and Winterton. The nucleate boiling heat transfer coefficient is calculated from the pool boiling correlation of Cooper [7]. Further, the convective heat transfer coefficient is based on the Dittus–Boelter correlation. Yoshida *et al*. [8] and Zhang *et al*. [9] both applied the Dittus–Boelter convective heat transfer correlation and the nucleate boiling correlation of Stephan and Abdelsalam [10] using their own proposed S factors.

In addition to models applying linear superposition, a model comprising a general power law has also been proposed and widely used :

$$h_{\mathrm{tp}} = \left(h_{\mathrm{nb}}^{\mathrm{n}} + h_{\mathrm{cv}}^{\mathrm{n}} \right)^{1/n} \tag{3}$$

where the exponent n is an empirical constant. Kutateladze [11] suggested using n = 2, whereas Steiner and Taborek [12] proposed power law models using $n = 3$.

In contrast to the superposition model that simultaneously considers the contributions of nucleate boiling, convective heat transfer, and their interactions, Shah [13] proposed the use of the maximum of the two values. In the Shah correlation, a dimensionless parameter N is introduced as a threshold. For different N values, various correlations are proposed to calculate the values of the nucleate boiling and convective coefficients. Subsequently, the higher value is chosen as the heat transfer coefficient of the two-phase fluid, as expressed in Eq. (4):

$$h_{tp} = \max\left(h_{nb}, h_{cv} \right) \tag{4}$$

Kandlikar [14] proposed a correlation similar to that of Shah in which h_{nb} and h_{cb} were revised on the basis of the single-phase convection correlation of Gnielinski [15]. In this correlation, similar to that of Shah [13], the convection number (Co), boiling number (Bo), and Froude number (F_r) are used to represent the convection and nucleate boiling parts.

Although there have been numerous studies of flow boiling prediction models for different refrigerants at different tube scales, it is very difficult to obtain a universal prediction model that can be applied to all the refrigerants because the flow boiling heat transfer characteristics are related to both the thermophysical properties of the refrigerant and the flow pattern. Saitoh *et al*. [16] measured the flow boiling heat transfer characteristics of HFO1234yf in a horizontal tube with inner diameter (ID) 2 mm and used a proposed Chen-type correlation by Saitoh *et al.* [17] that can be applied to low-pressure refrigerants like R134a. However, this correlation is not applicable to HFC32. Shin *et al*. [18] investigated the flow boiling heat transfer coefficient of several pure refrigerants and mixtures including pure HFC32 and HFC134a in a horizontal tube with ID 7.7 mm. They used a correlation proposed by Gungor and Winterton [19] to predict the heat transfer coefficient of these fluids. The average deviations of their prediction are 18.3% for HFC32 and 47.5% for HFC134a.

It is more difficult to predict the heat transfer coefficient of a refrigerant mixture than that of a pure refrigerant. For non-azeotropic refrigerant mixtures, which are the most commonly encountered, the saturation temperature increases during the evaporation process while decreases during the condensation process because each component has a different boiling point. The difference in the saturation temperature between the start and end points of the evaporation or condensation process at a constant pressure is called the temperature glide. Figure 1 shows an example of the temperature glides of HFO1234yf + HFC32 and R134a + HFC32 against the HFC32 mass fraction under the pressure at which the saturation temperature is 15 °C at a vapor quality of 0.5. Based on the measurement of Kamiaka *et al*. [20], the maximum temperature glides of HFO1234yf + HFC32 and R134a + HFC32 are 7.7 °C at a 22% mass fraction of HFC32 and approximately 6.1 °C at a 32% mass fraction of HFC32, respectively.

Previous analyses of the boiling heat transfers of non-azeotropic refrigerant mixtures have shown that the mass diffusion resistance of the mixture, which is the result of different boiling points, has a significant influence on the heat transfer. Figure 2 shows a schematic drawing of the mass diffusion when a bubble is generated in a binary mixture. A diffusion layer forms around the bubble because the components in the mixture have different boiling points, and the temperature and fraction of the mixture in the diffusion layer are different from those of the liquid bulk and saturation vapor. Scriven [21] developed the first analytical model for the bubble growth based on the energy balance and mass balance in a binary mixture. According to Scriven's model, the rate of bubble growth in a binary mixture is delayed due to the mass diffusion resistance. Van Stralen [22] proposed a model for a spherical bubble growing inside a binary liquid mixture which assumes that the composition gradient in the liquid surrounding the bubble retards the bubble growth. Van Wijk *et al*. [23] concluded that the effective superheat of a bubble growing in a binary mixture is less than that of a pure fluid with the same properties, because the saturation temperature at the bubble interface increases due to the accumulation of less-volatile components around the bubble.

For non-azeotropic mixtures, the typical approach for constructing predictive models is to modify the heat transfer correlation of pure fluids by considering the mass diffusion resistance. The mass diffusion resistance influences bubble growth related to the superheating of the liquid. Stephan and

Korner [24] noted that the maximum temperature difference occurs at the maximum $|\tilde{y}-\tilde{x}|$ of the mixture, where $\tilde{y}$ and $\tilde{x}$ are the mole fraction of volatile components in the vapor and liquid phase, respectively. They defined a real wall superheat ΔT that is the sum of the ideal superheat ΔT_{I} and the excess superheat ΔT^{E}, as expressed in Eq. (5). Factor A is a function of the type of mixture and is determined by Eq. (6). Note that the recommended A_0 value for acetone and ethanol is 0.75, whereas that of ethanol and benzene is 1.18. A value of 1.53 for A_0 is suggested if the composition of the mixture is unknown.

$$\Delta T = \Delta T_I + \Delta T^E = \tilde{x}_1 \Delta T_1 + \tilde{x}_2 \Delta T_2 + A \mid \tilde{y} - \tilde{x} \mid \Delta T_I \tag{5}$$

$$A = A_0 \left[0.88 + 0.12 \left(p/101325 \right) \right] \tag{6}$$

where ΔT_{i} is the difference between the wall temperature and the saturation temperature of component i (i = 1, 2) .

For predicting variations in the wall superheat based on the composition, Calus and Leonidopoulos [25] suggested an analytical expression

$$\Delta T = \left(\tilde{x}_1 \Delta T_1 + \tilde{x}_2 \Delta T_2 \right) \left[1 - \left(\tilde{y} - \tilde{x} \right) \left(\frac{a_c}{D_m} \right)^{1/2} \left(\frac{c_{\mathrm{pl}}}{\Delta h_{\mathrm{v}}} \right) \left(\frac{dT}{d\tilde{x}} \right) \right] \tag{7}$$

where D_{m} is the mass diffusion coefficient, a_{c} is the thermal diffusion factor, c_{pl} is the specific heat at a constant pressure in the liquid phase, Δh_{v} is the latent heat, and $dT/d\tilde{x}$ is the slope of the bubble point line.

Thome and Shock [26] postulated that the maximum rise in the local bubble temperature is equal to the temperature difference between the dew point and bubble point with the liquid feed composition. The heat transfer coefficient for the pool boiling of the mixture, h, is expressed as follows:

$$\frac{h}{h_{\mathrm{I}}} = \frac{\Delta T_{\mathrm{I}}}{\Delta T} = \frac{\Delta T_{\mathrm{I}}}{\Delta T_{\mathrm{I}} + \Delta T_{\mathrm{bp}}} \tag{8}$$

where h_{I} is the ideal heat transfer coefficient defined as $h_{\mathrm{I}} = 1 \Big/ \left[\left(\tilde{x}_1 / h_1 \right) + \left(\tilde{x}_2 / h_2 \right) \right]$.

The Chen correlation [3] is one of the most commonly adopted models for predicting the flow boiling heat transfer coefficients of pure refrigerants, and it also has been suggested as the basic method for mixtures if suitable corrections are applied. Based on this approach, Bennet and Chen [27] proposed the following correlation for mixtures and compared its predictions with the available data for ethylene glycol and water:

$$h_{\mathrm{tp}} = h_{\mathrm{ml}} F_{\mathrm{mix}} + h_{\mathrm{mnb}} S_{\mathrm{mix}} \tag{9}$$

They postulated that the heat transfer coefficient during nucleate boiling is related to the effective liquid superheat expressed by the Scriven equation [21]. Therefore, the suppression factor is expressed by the following equation:

$$S_{\mathrm{mix}} = S \frac{\Delta T_{\mathrm{mix}}}{\Delta T_{\mathrm{I}}} = S \left[1 - \left(\tilde{y} - \tilde{x} \right) \left(\frac{dT}{d\tilde{x}} \right) \left(\frac{c_{\mathrm{pl}}}{\Delta h_{\mathrm{v}}} \right) \left(\frac{a_c}{D_m} \right)^{0.5} \right]^{-1} \tag{10}$$

Jung *et al*. [28] studied azeotropic CFC12 + HFC152a refrigerant mixtures and compared the results with the data obtained for non-azeotropic HCFC22 + CFC114 mixtures. They proposed correlations based on the Chen correlation [3] and considered the mixture effects using only the phase equilibrium data. The mean deviations for the pure and mixed refrigerants were 7.2% and 9.6%, respectively. Zhang *et al*. [9] studied the flow boiling heat transfer coefficients of ternary mixtures (HFC32 + HFC125 + HFC134a) and modified the Yoshida *et al*. [8] correlation by adding correction factors to represent both nucleate boiling and forced convection. Mishra *et al*. [29] correlated their experimental data for R12 + R22 and reported coefficients for two different compositions as well as the revised factors for those mixtures. Bivens and Yokozeki [30] suggested a modification of both the Jung correlation [28] and the Wattelet correlation [31] to account for the mass transfer resistances of HFC32 + CFC12, HFC32 + HFC125, and HFC32 + HFC125 + HFC134a.

3 EXPERIMENTAL PROCEDURE

The test facility has been described in detail in Part I of this paper [2]. A pump cycle was used to measure the heat transfer coefficients of both the pure refrigerants and the refrigerant mixtures. The test section was a stainless steel tube with an inner diameter of 2 mm and wall thickness of 0.5 mm. The heat input for evaporation was provided by the Joule effect, and it can be assumed that the heat flux is constant along the tube length. The purity of the refrigerant HFO1234yf was 99.7% and that of HFC32 was 99.9%. HFO1234yf and HFC32 were mixed at the desired mass fraction in advance and charged into the system as liquid. The concentration of the mixture in the test tube was calculated on the basis of the fluid parameters measured at the inlet and outlet of the pre-heater using the Peng–Robinson-type equation of state proposed by Kamiaka *et al*. [20] and was confirmed using a gas chromatograph. The saturation temperature of the mixture at the vapor quality of 0.5 was set as 15 °C during the experiments. The local heat transfer coefficient h_{exp} in the test tube was defined as

$$h_{\mathrm{exp}} = \frac{q}{T_{\mathrm{wall}} - T_{\mathrm{sat}}} \tag{11}$$

where T_{wall} is the temperature of the inner wall and T_{sat} is the saturation temperature of the mixture or pure refrigerant, as deduced from the measured local refrigerant pressure.

The experimental conditions are summarized in Table 1. The data for pure HFO1234yf were taken from the measurements of Saitoh *et al*. [16]. The saturation vapor pressure of the mixture was very important for the saturation temperature, which is directly related to the temperature difference ($T_{\mathrm{wall}} - T_{\mathrm{sat}}T$) in Eq. (11). The vapor–liquid equilibrium properties of the mixtures were acquired using the Peng–Robinson-type state equation recommended by Kamiaka *et al*. [20]. The bubble and dew temperatures predicted by this new state equation agreed with the experimental results with a higher accuracy than in the case of REFPROP 8.0 [32], as shown in Fig. 2. The other properties of the HFO1234yf and HFC32 mixtures were obtained from the revised REFPROP 8.0 using the changed Peng–Robinson-type state equation. The properties of the pure refrigerants were calculated using REFPROP 8.0.

4 PREDICTION MODELS OF PRE-DRYOUT HEAT TRANSFER

Using the measurements in Part I [2], the variation in the heat transfer coefficients of the mixtures from the overall composition at similar vapor qualities was determined and is presented in Fig. 3. The variation between the heat transfer coefficient and the HFC32 concentration is not linear. Shin *et al*. [18] claimed that this is because of nonlinear variations in the thermophysical properties of a mixture, such as the viscosity, thermal conductivity, surface tension, density of the liquid and vapor phases, and other properties, with respect to the overall composition and mass transfer resistance at the vapor–liquid interface of a non-azeotropic mixture.

In this study, a prediction model for two pure refrigerants—HFO1234yf and HFC32—is developed, as well as a correlation for the prediction of the refrigeration mixture.

4.1 Boiling Heat Transfer Coefficient vs. Lockhart–Martinelli Parameter

Typically, the flow boiling heat transfer in a tube is calculated as a superposition of the nucleate boiling heat transfer and the forced convective evaporation. At the region dominated by the forced convective evaporation, the flow boiling data can be correlated by the relation $h_{\mathrm{exp}} \propto h_l(1/\mathrm{X_{tt}})^{\mathrm{n}}$, where h_l is the heat transfer coefficient for the liquid flow alone and $\mathrm{X_{tt}}$ is the Lockhart–Martinelli parameter. The magnitude of the forced convective evaporation can thus be represented by gradient n of the linear regression applied to the experimental data. Figure 5 shows logarithmic plots of the measured heat transfer coefficients against $1/\mathrm{X_{tt}}$ for HFC32, HFO1234yf, and HFO1234yf + HFC32 (80/20 and 50/50 by mass%) in the pre-dryout region. Clearly, most of the data can be fitted to the relation $h_{\mathrm{exp}}/h_l \propto (1/\mathrm{X_{tt}})^{\mathrm{n}}$, where the exponent n lies between 0.55 and 0.75. It can also be seen in Fig. 5 that the values of h_{exp}/h_l are similar for pure refrigerants or mixtures when the sets of the mass flux and heat flux have the same proportional relationship. For example in the cases of a mass flux of 400 kg/m^{2}s and a heat flux of 12 kW/m^2 and a mass flux of 200 kg/m^{2}s and heat flux of 6 kW/m^2. The Bo, as shown in Eq. (12), can depict the relative importance of nucleate boiling against convective heat transfer in flow boiling heat transfer, and the interaction between them. At a high Bo, nucleate boiling absolutely dominates the heat transfer, as in a case with a mass flux of 200 kg/m^{2}s and

heat flux of 24 kW/m^2. Although it has the same Reynolds number as the case with a mass flux of 200 kg/m^{2}s and heat flux of 6 kW/m^2, the h_{exp}/h_l value of the former is much higher than that of the latter.

$$Bo = \frac{q}{h_{\mathrm{lv}} G} \tag{12}$$

4.2 Prediction of Heat Transfer Coefficient of Pure HFO1234yf and HFC32

4.2.1 Existing correlations for pure fluids

Several correlations have been proposed to predict the heat transfer coefficients of pure HFO1234yf and HFC32. The details of the correlations compared in this study are summarized in the Appendix. Most of the correlations have adopted the form of Chen's correlation, which includes two parts: a nucleate boiling term and convective heat transfer term. The Dittus–Boelter correlation, Eq. (A.3), generally has been accepted to calculate the convective heat transfer of a fluid. The Stephan–Abdelsalam correlation [10], as expressed in Eq. (A.8), is used to calculate the nucleate boiling heat transfer coefficient. Based on the Dittus–Boelter correlation (Eq. (A.3)) and the Stephan–Abdelsalam correlation (Eq. (A.8)), Yoshida *et al*. [8], Zhang *et al*. [9], and Saitoh *et al*. [17] predicted two-phase fluid evaporation heat transfer coefficients by introducing a new suppression factor *S* and an enhancement factor *F*. Yoshida *et al*. suggested that the expression of *S* should include not only the effect of local two-phase Reynolds number but also of the boiling number. Saitoh *et al*. [16] used their correlation to predict the heat transfer coefficient of HFO1234yf and obtained high prediction accuracies. In their correlation, a Weber number was introduced into factor *F* to represent the effects of small tube diameters on the heat transfer performance, as shown in Eq. (A.13). Gungor and Winterton [19] developed a simplified correlation of the Chen form, as expressed in Eq. (A.18). Except for the correlation of Gungor and Winterton, all the correlations use the function $F = f\left[\left(1/X_{tt}\right)^n\right]$ as the *F* factor. Shah's correlation [13] is also a popular correlation to predict the heat transfer coefficients of refrigerants.

Figures 6 (a) and (b) show comparisons of the experimental results and the results predicted for pure HFO1234yf using the six abovementioned correlations. The experimental data for pure HFO1234yf are best fitted by the correlations proposed by Saitoh *et al*., Shah, and Chen. Some of the data predicted by the correlation of Yoshida *et al*. exceed the deviation limit of 20% but are still within 25%. The correlations of Zhang *et al*. [9] and Gunger and Winterton [19] slightly overestimate the experimental results for pure HFO1234yf but the deviations are less than 35% on average. Figures 6 (c) and (d) show the comparison for pure HFC32. From the correlations of Yoshida *et al*. [8], Chen [3], Zhang *et al*. [9], and Gungor and Winterton [19], 80% of the experimental points are captured with deviations in the range of ±20%. The tendencies of the results by Saitoh *et al*. and Shah are similar and the deviations of most of the prediction data are greater than 20%. Figures 6 (b) and (d) show that the results evaluated with the correlations of Gunger and Winterton [19] change slightly under different conditions. Hence, the prediction tendency is different from that of the experimental data.

4.2.2 Model proposed for pure refrigerants

Based on the measured pre-dryout heat transfer coefficients for both pure refrigerants and refrigerant mixtures, a new correlation is proposed following Chen's correlation, as shown in Eq. (13). The nucleate boiling heat transfer form is the correlation proposed by Cooper [7] because it can predict the heat transfer coefficient of refrigerants with high accuracy. The forced convective heat transfer correlation, Eq. (15), is calculated using the Dittus–Boelter equation. In factor *F*, we applied the similar correlation proposed by Saitoh *et al*. [17], in which a Weber number is introduced to consider the effect of the surface tension on flow patterns at different tube diameters. Saitoh *et al*. [17] introduced the Weber number based on experimental data with an inner tube diameter from 0.51 to 10.92 mm; compared to that of gravity and inertia force, the effect of surface tension on a two-phase flow becomes more significant as the tube diameter decreases. However, the correlation proposed by Yoshida *et al*. [8] was based on experimental data with an inner tube diameter from 4.8 mm to 16.9 mm, in which the effect of surface tension on flow pattern is negligible. Because this paper discusses the flow boiling heat transfer characteristics at a relatively small tube diameter of 2 mm, it is reasonable to introduce the Weber number into our proposed factor *F*. The exponent *n* in factor *F* is taken as 0.88, i.e., the same as the value recommended by Yoshida *et al*. [8]. In Fig. 5, the h_{tp}/h_l at a

high vapor quality (large $1/X_{tt}$) under various conditions can be unified. This means that when the convective heat transfer dominates the whole heat transfer, the $h_{tp} \propto h_l(1/\mathrm{X_{tt}})^{\mathrm{n}}$. The maximum exponent n in Fig. 5 is 0.72, which is close to the value of 0.88 proposed by Yoshida *et al.* [8] but far less than the value of 1.05 proposed by Saitoh *et al.* [17]. The exponent n is therefore set to be 0.88 to be consistent with Yoshida's correlation because Yoshida's correlation was proposed under a wider range of experimental conditions and using different refrigerants.

The *Bo* number is introduced into the function of S, similar to that of Yoshida *et al*. [8], because experimental results indicate that some regulations of the heat transfer coefficient under various conditions are related to the *Bo* number. In Yoshida's correlation, both Re_{tp} and X_{tt} are used to reflect the effect of the acceleration of the vapor on the boiling. However, $Re_{tp} = Re_l F^{1.25}$, which also includes X_{tt}. To simplify the correlation, the X_{tt} is not used explicitly, but only the Re_{tp} is applied in S to express the influence of convective heat transfer on nucleate boiling by selected proper constants based on our experimental results. These constants, therefore, are different from those in the factor S proposed by Yoshida *et al*.

$$h_{\mathrm{tp}} = Sh_{nb} + Fh_{CV} \tag{13}$$

$$h_{\mathrm{nb}} = 55\, p_r^{0.12} \left(-\log p_r\right)^{-0.55} M^{-0.5} q^{0.67} \tag{14}$$

$$h_{\mathrm{cv}} = 0.023 \frac{\lambda_{\mathrm{l}}}{d}\left[\frac{G\left(1-x\right)d}{\mu_{\mathrm{l}}}\right]^{0.8} \mathrm{Pr}^{0.4} \tag{15}$$

$$F = 1.0 + 1.8\left(0.3 + 1/X_{\mathrm{tt}}\right)^{0.88} \Big/ \left(1 + We_{\mathrm{v}}^{-0.4}\right) \tag{16}$$

$$S = \frac{1}{0.5 + 0.5\dfrac{\left(\mathrm{Re}_{\mathrm{tp}} \times 10^{-3}\right)^{0.3}}{\left(Bo \times 10^{3}\right)^{0.23}}} \tag{17}$$

Figure 7 shows a comparison of the prediction results obtained by the proposed correlation with the experimental results for different refrigerants, under different mass flux and heat flux conditions. Figure 7 (a) shows the comparison results for HFO1234yf with different heat fluxes while a constant mass flux is maintained. As the heat flux increases, the predicted results also increase in a manner similar to the measured results. When the heat flux is 24 kW/m^2, the proposed model slightly overestimates the experimental results at high vapor qualities. Figure 7 (b) shows the results for HFO1234yf at different mass fluxes while a constant heat flux is maintained. The heat transfer coefficient increases monotonically with the vapor quality when the mass flux becomes large. This result obeys the rule that the heat transfer is basically dominated by nucleate boiling at low vapor qualities and by forced convection at high vapor qualities or large mass fluxes. The correlation represents the trend in the heat transfer coefficients quite well but slightly overestimates the values by approximately 10% on average.

Comparisons of the measured results and predicted results based on the proposed correlation for HFC32 at identical mass and heat fluxes are shown in Fig. 7 (c) and Fig. 7 (d), respectively. Similar to the case of HFO1234yf, the results estimated for HFC32 almost follow the variations in the trend for the experimental data. From these two figures, the correlation slightly underestimates the measured heat transfer coefficients when the mass flux is 200 kg/m^{2}s and the heat flux is 24 kW/m^2, but underestimates by a higher magnitude of 22% on average, when the mass flux is 100 kg/m^{2}s and the heat flux is 12 kW/m^2.

Figure 8 shows direct comparisons of the predicted and measured results for pure HFO1234yf and pure HFC32. The deviation limit of the proposed correlation for these pure refrigerants is less than ±20% for 85% of the data.

4.2.3 Accuracy of proposed correlation

To compare the accuracies of the prediction methods with the data in the experimental database, the deviation is defined by the relative mean absolute error as follows:

$$\mathrm{RMAE} = \frac{1}{n}\sum_{i=1}^{n}\left|\frac{h_{\mathrm{exp},i} - h_{cal,i}}{h_{\mathrm{exp},i}}\right| \tag{18}$$

From the comparisons in Tables 2 and 3, the best fitting correlations for pure HFC32 and pure HFO1234yf are those proposed in this study. Moreover, acceptable prediction results are obtained by the correlations of Yoshida *et al*. [8] and Chen [3]. Although the correlations of Zhang *et al*. [9] and Gunger and Winterton [19] can accurately predict the heat transfer coefficient of HFC32, they show errors in the trend for the heat transfer coefficient of HFO1234yf. The predicted results of the correlation proposed by Saitoh *et al*. [17] are in good agreement with the results obtained for pure HFO1234yf but exhibit the worst fit with those for pure HFC32.

4.3 Prediction Model for Refrigerant Mixtures

4.3.1 Existing correlations for mixtures of HFO1234yf and HFC32

In this study, we first presumed that the mass diffusion resistance is negligible; therefore the correlation proposed for pure refrigerant can be applied to the prediction of refrigerant mixture as long as the average properties of the mixture are properly employed. The correlations proposed by Yoshida *et al*. [8], Chen [3], Zhang *et al*. [9], Shah [13], and the present study for pure refrigerants were employed to predict the heat transfer coefficients of the HFO1234yf + HFC32 (80/20 and 50/50 by mass%) mixture using the average properties of the mixtures.

In addition, we verified the applicability of three models proposed for different refrigerant mixtures to the HFO1234yf + HFC32 refrigerant mixtures. Mishra *et al*. [29] developed a correlation based on their data for R12 + R22, as expressed in Eq. (A.21). In this correlation, the factors *C*, *m*, and *n* are constants based on the mass fraction of R12. Sami *et al*. [33] developed a correlation expressed in Eq. (A.22) for mixtures in enhanced tubes. Bivens and Yokozeki [30] considered the effects of the mass transfer resistance on the heat transfer of the HFC32 + HFC125 and HFC32 + HFC125 + HFC134a mixtures and suggested modifications to the Jung correlation [28] and the Wattelet correlation [31].

Figure 9 shows the measured results and the results estimated by the seven correlations for the HFO1234yf + HFC32 (80/20 and 50/50 by mass%) mixtures. Figures 9 (a) and (b) show that the correlations of Mishra *et al*. [29] and Sami *et al*. [33] both underestimate the measured heat transfer coefficients of HFO1234yf + HFC32 (80/20 and 50/50 by mass%). The correlation of Bivens and Yokozeki [30] also overestimates the results for HFO1234yf + HFC32 (80/20 by mass%). However, most of the results predicted for HFO1234yf + HFC32 (50/50 by mass%) are within the deviation limit of ±20%.

Figure 9 (c) shows that most of the results predicted by the correlations of Yoshida *et al*. [8], Chen [3], Zhang *et al*. [9], and the present study exceed the deviation limit of ±20%. This means that the measured heat transfer coefficients of the mixtures are lower than those calculated using the correlations for pure refrigerants. However, the four correlations are in good agreement with the heat transfer coefficient of HFO1234yf + HFC32 (50/50 by mass%), as shown in Fig. 9 (d). The temperature glide of the HFO1234yf + HFC32 (50/50 by mass%) mixture is about 4.5 ^{o}C at the test saturation pressure of 1.06 MPa. Because of the large temperature glide of the HFO1234yf + HFC32 (80/20 by mass%) mixture—about 7.4 ^{o}C at a test saturation pressure of 0.77 MPa—and the existence of mass diffusion resistance, the evaporative heat transfer of the mixture was drastically suppressed. Hence, the predicted results are not sufficient when only the average properties of the mixture are considered. According to the analysis of Scriven [21] and Van Stralen *et al*. [22], the gradient of the concentration in a binary mixture will lead to the suppression of the boiling heat transfer. Although the influence of mass diffusion is considered in the correlations of Mishra *et al*. [29], Sam *et al*. [33], and Bivens and Yokozeki [30], these three correlations for the mixtures cannot produce a good fit to the heat transfer coefficients of the HFO1234yf + HFC32 (80/20 by mass%) mixture, as shown in Table 4.

A detailed comparison of the results of the seven correlations listed in Tables 4 and 5 indicates that the correlations of Yoshida *et al*. [8], Chen [3], Zhang *et al*. [9], and the present study must be improved to obtain reasonable predictions for refrigerant mixtures with a relatively large temperature glide. Further, new suppression factors must be introduced into the correlations to reflect the suppressions caused by the concentration distribution.

4.3.2 Characteristics of flow boiling heat transfer in mixtures

In a manner similar to that of pure fluids, the flow boiling heat transfer of a mixture also occurs owing to the interaction of nucleate boiling and convective heat transfer. Figure 2 clearly shows that mass diffusion exists and affects the heat transfer coefficients of mixtures during the nucleate boiling process. Mass diffusion also exists during the convective heat transfer process, as shown in Fig. 10. In convection heat transfer, the main flow pattern is annular flow and the convective evaporation process occurs at the liquid–vapor interface. Because the components in the liquid mixture have different evaporation rates, it is considerably easier for a volatile component to escape from the interface. A composition gradient layer forms near the interface, and the volatile component in the liquid bulk has to pass through the diffusion layer before arrives at the interface, thereby affecting the heat transfer coefficient of the fluid. Therefore, for a mixture, the heat transfer coefficients are affected not only by the interaction between the nucleate boiling and convective heat transfer, but also by the mass transfer resistance inside the diffusion layer.

In addition, the test results of Li *et al*. [2] indicate that the mass diffusion resistance is also related to the *Bo* number. Comparing the heat transfer coefficient of a mixture to that of a pure refrigerant against the vapor quality at high and low *Bo* values shows that, at a high *Bo*, the heat transfer of the mixture deteriorates across the entire pre-dryout region, whereas at a low *Bo*, the deviation of the heat transfer coefficient of the mixture increases with an increase in vapor quality.

At a high *Bo*, nucleate boiling dominates the entire heat transfer, with a high heat flux causing violent boiling. Because of the high density of bubbles on the surface, the boundary layers of two bubbles may overlap each other, as shown in Fig. 11 (a). It is more difficult for the volatile component to reach the interface, and a larger compositional inhomogeneity forms in the interface around the bubble. Compared to the influence of heat flux on the form of the mass diffusion layer, the disturbances in the fluid caused by the mass flux are too weak to decrease the mass diffusion resistance effectively.

When *Bo* is low, at a high vapor quality, the convective heat transfer dominates the entire heat transfer. Because of the acceleration of the vapor phase, the velocity of the liquid phase increases, and nucleate boiling is suppressed completely. Subsequently, evaporation occurs violently at the interface of the liquid and vapor phases, not at the surface of the bubble. According to the same principle of evaporation, the volatile component evaporates first through the interface, and a concentration gradient layer forms near the interface, as shown in Fig. 11 (b). The volatile component in the bulk has to pass through this layer to complement the content of the volatile component attributable to the concentration gradient. Although a large mass flux can help eliminate the concentration gradient, the mass diffusion still affects the convective heat transfer owing to the strong compositional inhomogeneity during the intense evaporation process.

At moderate *Bo* values, both the nucleate boiling and convective heat transfer contributes to the flow boiling heat transfer, a concentration gradient layer exists at not only the surface of the bubble, but also at the liquid and vapor phase interface, as shown in Fig. 11 (c). Because the bubble density is low, it is easy to complement the volatile component from the bulk to the interface, and the compositional inhomogeneity is decreased in comparison to that at a high *Bo*. The component gradient near the evaporation interface is low because the evaporation process is less vigorous. Moreover, a bubble transitioning from the liquid phase to the vapor phase can cause agitation, which decreases the effect of the mass diffusion.

These results imply that at a high *Bo*, the heat transfer deteriorates mainly because of the mass transfer resistance for the nucleate boiling, whereas at a low *Bo*, the effect of the mass transfer resistance on the convective heat transfer is more remarkable than that on the nucleate boiling.

4.3.3 Model proposed for mixtures of HFO1234yf and HFC32

As noted in section 4.3.2, the mass diffusion resistance influences the nucleate boiling and convective heat transfer by different degrees under various conditions. Therefore, revising factors are introduced into the prediction correlation of pure refrigerants to predict the heat transfer coefficient of the mixture. Two suppression factors—F_{mix} and S_{mix}—are introduced into Chen's correlation (Eq. 13) to reflect the influence of the mass diffusion resistance on both the convective heat transfer and nucleate boiling, as shown in Eqs. (19–21).

$$h_{\mathrm{tp}} = F_{\mathrm{mix}} F h_{\mathrm{cv}} + S_{\mathrm{mix}} S h_{\mathrm{nb}} \tag{19}$$

$$F_{\mathrm{mix}} = \exp\left(-0.027\left(T_{\mathrm{m,sat}} - T_{\mathrm{b}}\right)\right) \tag{20}$$

$$S_{\mathrm{mix}} = \frac{\Delta T_{\mathrm{m}}}{\Delta T_{\mathrm{id}}} = \left[1 - \left(\tilde{y} - \tilde{x}\right)\left(\frac{dT}{d\tilde{x}}\right)\left(\frac{c_{\mathrm{pl}}}{\Delta h_{\mathrm{v}}}\right)\left(\frac{a_c}{D_m}\right)^{0.5}\right]^{-1} \tag{21}$$

In forced convective boiling, the evaporating process mainly occurs at the vapor–liquid interface, as shown in Fig. 10. The mole fraction difference, $\tilde{y} - \tilde{x}$, which relates to the difference between the interface temperature and saturation temperature, is a very important driving force to influence the mass diffusion. Many previous studies have applied either $C|\tilde{y} - \tilde{x}|$ or $1 - C|\tilde{y} - \tilde{x}|^{\mathrm{n}}$ to correct the heat transfer coefficient of a mixture. For example, Sami *et al*. [33] used the correlations of $h = 0.155(\lambda_{\mathrm{l}}/D)ARe^{0.62}\lambda_{\mathrm{l}}^{0.3}$ where $A = 1 - C(\sum|\tilde{y} - \tilde{x}|)^{0.82}$, and Shin *et al*. [34] used $h/h_{\mathrm{l}} = (1 - C_{\mathrm{F}})F$, where F is Chen's two-phase correction factor and $C_{\mathrm{F}} = A|\tilde{y} - \tilde{x}|^{\mathrm{n}}$. Because it is not easy to obtain the interface temperature, in this study, we used the temperature difference between the bulk temperature and bubble point temperature of the fluid to correct the forced heat transfer coefficient. The F_{mix} formula is similar to the equation of Palen and Small [35], but the definition of the temperature difference is not the same. In Palen and Small's correlation of Eq. (22),

$$h/h_{\mathrm{l}} = \exp\left(-0.027\left(T_{\mathrm{bi}} - T_{\mathrm{b0}}\right)\right) \tag{22}$$

the term $(T_{\mathrm{bi}} - T_{\mathrm{b0}})$ is the temperature difference between the vapor leaving a reboiler and the liquid feed to it. As the vapor quality incrementally increases, the convective heat transfer intensifies gradually; thus, the mass diffusion resistance near the vapor–liquid interface of convective heat transfer significantly rises with the concentration gradient, which is similar to the situation shown in Fig. 11 (b). The temperature of the fluid deviates from the previous saturation temperature because of this concentration gradient. In the proposed F_{mix} of Eq. (20), the difference of the saturation temperature of the mixture (T_{satm}) and the bubble point temperature of the mixture (T_{b}) is applied; this value increases gradually in the evaporation process to cause a decrease in F_{mix} to suppress the convective heat transfer.

S_{mix} is given by the formula of Scriven [21], who investigated the influence of mass transfer on the growth of a spherical bubble in a binary mixture. The equation by Scriven describes the difference of bubble growth in the nucleate boiling of pure materials and binary mixtures, as shown in Eq. (23).

$$R = R_{pure}\left[1 - \left(\tilde{y} - \tilde{x}\right)\left(\frac{dT}{d\tilde{x}}\right)\left(\frac{c_{\mathrm{pl}}}{\Delta h_{\mathrm{v}}}\right)\left(\frac{a_c}{D_m}\right)^{0.5}\right]^{-1} \tag{23}$$

The growth of a bubble is related to the superheat of the fluid. The superheat required to grow a bubble in a binary mixture is different from that in a pure fluid. Bennet and Chen [27] suggested that the deterioration of the heat transfer coefficient during nucleate boiling in a mixture is due to the greater superheat required for a mixture than for a fluid without mass diffusion resistance. They proposed a suppression factor S_{mix} of the ratio of the effective liquid superheat to the ideal superheat; this factor is equal to that of the Scriven equation, as shown in Eq. (21). For this equation, it is difficult to obtain the mass diffusion coefficient D_m; hence, the hard sphere model for the diffusion coefficients of the components in a binary solution proposed by Kenneth *et al*. [36] is used, as shown in Eqs. (24)–(26).

$$D_{\mathrm{m}} = D_{\mathrm{kin}}\left[1 + \left(\partial \ln \gamma_1 / \partial \ln \tilde{x}_1\right)_{\mathrm{T,P}}\right] \tag{24}$$

$$D_{\mathrm{kin}} = D_{\mathrm{kin}}^{\mathrm{Ens}} AC\left(\eta, \frac{m_1}{m_2}, \frac{\tilde{\sigma}_1}{\tilde{\sigma}_2}, \tilde{x}_1\right) \tag{25}$$

$$C\left(\eta, \frac{m_1}{m_2}, \frac{\tilde{\sigma}_1}{\tilde{\sigma}_2}, \tilde{x}_1\right) \approx \tilde{x}_1 C\left(\eta, \frac{m_1}{m_2}, \frac{\tilde{\sigma}_1}{\tilde{\sigma}_2}, 1\right) + \tilde{x}_2 C\left(\eta, \frac{m_1}{m_2}, \frac{\tilde{\sigma}_1}{\tilde{\sigma}_2}, 0\right) \tag{26}$$

where D_{m} is the mass diffusion coefficient, and D_{kin} is the kinetic diffusion coefficient defined by Kenneth *et al.* [36]. $D_{\mathrm{kin}}^{\mathrm{Ens}}$ is the Enskog transport equation for the kinetic mutual diffusion coefficient, which is only valid for the fluid of a smooth hard sphere. Factors A and C are introduced to correct the

neglected part in Enskog theory. A detailed explanation for the corrected factor is given in the Appendix.

The activity coefficient (γ) and fugacity of the mixture are required in the calculation. Hence, they are evaluated using REFPROP Ver. 8.0. The fugacity is the effective pressure of a real gas. The predicted mass diffusion coefficient of HFO1234yf + HFC32 is approximately 2×10^{-5} cm^2/s during the evaporation process, as shown in Fig. 12.

The suppression factors for the mixture, S_{mix} and F_{mix}, are introduced into the correlations for pure refrigerants, i.e., the correlations of Yoshida *et al*. [8], Chen [3], Zhang *et al*. [9], and the present study.

Figure 13 shows the comparison of experimental results with the predicted values for the HFO1234yf + HFC32 (80/20 and 50/50 by mass%) mixtures using the proposed model with the suppression factors for the mixtures. Figure 13 (a) shows that the measured heat transfer coefficient of the HFO1234yf + HFC32 (80/20 by mass%) mixture increases monotonically with the vapor quality at a mass flux of 200 kg/m^{2}s and heat flux ranging from 6 to 24 kW/m^2. The correlation predicts both the trend and magnitude (10% difference) of the heat transfer coefficient. Figure 13 (b) shows the results for the HFO1234yf + HFC32 (80/20 by mass%) mixture at a heat flux of 12 kW/m^2, with the mass flux ranging from 100 to 400 kg/m^{2}s. The correlation overestimates the heat transfer coefficient at high and low mass fluxes by approximately 20%. Figures 13 (c) and (d) compare the measurements with the predictions for the HFO1234yf + HFC32 (50/50 by mass%) mixture. Figure 13 (c) shows the results when the heat flux is varied from 6 to 24 kW/m^2 while the mass flux is maintained at 200 kg/m^{2}s. The entire trend for the measured heat transfer coefficient versus vapor quality becomes moderate as the heat flux increases. The correlation captures this trend when the heat flux changes. Figure 13 (d) shows the results when the mass flux varies from 100 to 400 kg/m^{2}s while the heat flux is maintained at 12 kW/m^2. The moderate increase of heat transfer coefficient against vapor quality at a mass flux of 100 kg/m^{2}s turns to a steep increase at a mass flux of 400 kg/m^{2}s. The correlation accurately predicts the trends with the changes in the mass flux, and the absolute values of the heat transfer coefficients are captured by the correlation with an average deviation of less than 10%.

Tables 6 and 7 list the relative mean deviations of the results predicted for HFO1234yf + HFC32 (80/20 and 50/50 by mass%) using the suppression factors in these four correlations for pure refrigerants. When the F_{mix} and S_{mix} factors were introduced for the mixture, the prediction accuracies of the four correlations improved. The correlation proposed in this study outperforms the others for the heat transfer coefficient predictions for the mixture, but slightly overestimates the values under some conditions, such as the case with a mass flux of 100 kg/m^{2}s and heat flux of 12 kW/m^2, with an average deviation less than 20%. The results predicted using the correlations of Yoshida *et al*. [8] and Chen [3] are also acceptable after the introduction of suppression factions.

5 PREDICTION OF PRESSURE DROP

The pressure drop of flow boiling includes two parts in a horizontal tube: the friction pressure drop and momentum pressure drop. The pressure drop caused by the acceleration of vapor is calculated by using Eq. (38) as recommended by Thome [37]. ε is the void fraction, which is calculated by Eq. (39) [38]. The friction pressure drops for the pure refrigerants HFO1234yf and HFC32 and the HFO + HFC32 mixtures with two concentrations were predicted using five separated flow models: the models of Grönnerud [39], Lockhart–Matinelli [40], Müller-Steinhagen and Heck [41], and Friedel [42], which were developed for macrochannels, and the Hwang and Kim correlation [43] that was developed for microchannels. The mean absolute errors of these models are shown in Table 8. The model proposed by Müller-Steinhagen and Heck outperformed the other models. Figure 14 shows comparisons of the experimental results and the predicted total pressure drop obtained using the momentum pressure drop model (Eq. 38) and the friction pressure drop model of Müller-Steinhagen and Heck [41]. This method captured 80%–90% of the experimental results for HFO1234yf and the two mixtures within a deviation of ±30%. Among the results for HFC32 predicted by the Müller-Steinhagen and Heck correlation exhibited the best agreement with the experimental data within a deviation limit of ±30%. The Lockhart–Matinelli correlation also accurately predicted the data for HFO1234yf and the mixtures, but in the case of HFC32, the deviation was over ±30%. The correlation of Hwang and Kim for microchannels overestimated the results compared to the experimental data.

$$\Delta p_{\mathrm{mom}} = m_{\mathrm{f}}^2 \left\{ \left[\frac{(1-x)^2}{\rho_{\mathrm{l}}(1-\varepsilon)} + \frac{x^2}{\rho_{\mathrm{v}}\varepsilon} \right]_{\mathrm{out}} + \left[\frac{(1-x)^2}{\rho_{\mathrm{l}}(1-\varepsilon)} + \frac{x^2}{\rho_{\mathrm{v}}\varepsilon} \right]_{\mathrm{in}} \right\} \tag{38}$$

$$\varepsilon = \frac{x}{\rho_{\mathrm{v}}} \left[(1+0.12(1-x)) \left(\frac{x}{\rho_{\mathrm{v}}} + \frac{(1-x)}{\rho_{\mathrm{l}}} \right) + \frac{1.18(1-x)\left[g\sigma(\rho_{\mathrm{l}} - \rho_{\mathrm{v}}) \right]^{0.25}}{m_{\mathrm{f}}^2 \rho_{\mathrm{l}}^{0.5}} \right]^{-1} \tag{39}$$

6 CONCLUSIONS

Predictions were performed based on experiments on the flow boiling heat transfer of pure HFO1234yf, HFC32, and the HFO1234yf + HFC32 (80/20 and 50/50 by mass%) refrigerant mixture in a 2 mm smooth tube. The results are summarized as follows:

(1) Several existing correlations were applied to predict the heat transfer coefficients of pure HFO1234yf, HFC32, and HFO1234yf + HFC32 (80/20 and 50/50 by mass%). The correlations of Yoshida *et al*. and Chen predicted the heat transfer coefficient of HFO1234yf and HFO1234yf + HFC32 (50/50 by mass%) with acceptable accuracy. However, these two correlations underestimated the heat transfer coefficients of HFC32 under some conditions.

(2) A new semi-empirical correlation based upon the superposition of the contributions from nucleate boiling and convection was in very good agreement with the magnitudes and trends of the heat transfer coefficients of pure HFO1234yf, HFC32, and HFO1234yf + HFC32 (50/50 by mass%) with a relative mean absolute error of approximately 20%. The average properties of the mixture were used in the calculation.

(3) The existing correlations and the proposed correlation overestimated the heat transfer coefficient of HFO1234yf + HFC32 (80/20 by mass%) with a large temperature glide of 7.4 $^{\mathrm{o}}$C at the test saturation pressure because of the effects of mass diffusion resistance.

(4) Suppression factors were proposed for the mixture and introduced into both the existing correlations and the newly proposed correlation. The prediction accuracies of these correlations were improved for the HFO1234yf + HFC32 (80/20 and 50/50 by mass %) mixture. The absolute values of the heat transfer coefficients obtained by the proposed correlation have an average deviation of less than 20%.

(5) The correlation proposed by Müller-Steinhagen and Heck [41] can predict the pressure drops of the mixtures and pure HFO1234yf and HFC32. In the case of the predicted results for the HFO1234yf + HFC32 mixtures, 80%–90% are in good agreement with the measured pressure drops within a deviation of ±30%.

ACKNOWLEDGMENTS

This study was sponsored by the "Development of Non-fluorinated Energy-Saving Refrigeration and Air Conditioning Systems" project of the New Energy and Industrial Technology Development Organization of Japan. The first author is grateful for the financial support received from the Japan Society for the Promotion of Science (JSPS) and NSFC No. 51176133 and 50976075.

APPENDIX

(1) Correlations of Chen [3]:

$$h_{\mathrm{tp}} = Sh_{\mathrm{n}} + Fh_{\mathrm{l}} \tag{A.1}$$

$$h_{\mathrm{n}} = 0.00122 \left(\frac{\lambda_{\mathrm{l}}^{0.79} {c_{p\mathrm{l}}}^{0.5} \rho_{\mathrm{l}}^{0.49}}{\sigma^{0.6} \mu_{\mathrm{l}}^{0.29} h_{\mathrm{lv}}^{0.24} \rho_{\mathrm{v}}^{0.24}} \right) \left[t_{\mathrm{w}} - t_{\mathrm{sat}}(p_{\mathrm{l}}) \right]^{0.4} \left[p_{\mathrm{sat}}(t_{\mathrm{w}}) - p_{\mathrm{l}} \right]^{0.75} \tag{A.2}$$

$$h_{\mathrm{l}} = 0.023 \,\mathrm{Re}_{\mathrm{l}}^{0.8} \,\mathrm{Pr}_{\mathrm{l}}^{0.4} \,\lambda / d \tag{A.3}$$

$$\mathrm{Re}_{\mathrm{l}} = G(1-x)d / \mu_{\mathrm{l}} \tag{A.4}$$

$$S = \frac{1}{1+\left(2.56\times10^{-6}\right)\left(\mathrm{Re_l}\,F^{1.25}\right)^{1.17}} \tag{A.5}$$

$$F = 1.0, X_{\mathrm{tt}} \geq 10 \tag{A.6}$$

$$F = 2.0\left(0.213 + 1/X_{\mathrm{tt}}\right)^{0.736}, X_{\mathrm{tt}} < 10 \tag{A.7}$$

(2) Correlations of Yoshida *et al*. [8]:

$$h_{\mathrm{n}} = 207\frac{\lambda_{\mathrm{l}}}{d_{\mathrm{b}}}\left(\frac{qd_{\mathrm{b}}}{\lambda_{\mathrm{l}}T_{\mathrm{l}}}\right)^{0.745}\left(\frac{\rho_{\mathrm{v}}}{\rho_{\mathrm{l}}}\right)^{0.581}\mathrm{Pr_l}^{0.533} \tag{A.8}$$

$$d_{\mathrm{b}} = 0.51\left[\frac{2\sigma}{g\left(\rho_{\mathrm{l}}-\rho_{\mathrm{v}}\right)}\right]^{0.5} \tag{A.9}$$

$$F = 1 + 2\left(1/X_{\mathrm{tt}}\right)^{0.88} \tag{A.10}$$

$$S = 1\Big/\left\{1+0.9\left[\left(\mathrm{Re_{tp}}\times10^{-4}\right)^{0.5}\Big/\left(\left(Bo\times10^{4}\right)\times X_{\mathrm{tt}}{}^{0.5}\right)\right]\right\} \tag{A.11}$$

$$Bo = q/Gh_{lv} \tag{A.12}$$

(3) Correlations of Saitoh *et al*. [17]:

$$F = 1+\left(1/X_{\mathrm{tt}}\right)^{1.05}\Big/\left(1+We_{\mathrm{v}}{}^{-0.4}\right) \tag{A.13}$$

$$S = 1\Big/\left[1+0.4\left(Re_{\mathrm{tp}}\times10^{-4}\right)^{1.4}\right] \tag{A.14}$$

$$\mathrm{Re_{tp}} = \mathrm{Re_l}F^{1.25} \tag{A.15}$$

(4) Correlations of Zhang *et al*. [9]:

$$F = 1 + 2\left(1/X_{\mathrm{tt}}\right)^{0.88} \tag{A.16}$$

$$S = \frac{1}{1+0.4(\mathrm{Re_{tp}}\times0.0001)^{0.5}/\left(\dfrac{q\times10000}{G\times h_{\mathrm{lv}}}\right)^{0.5}\left(\dfrac{1}{X_{tt}}\right)^{0.5}} \tag{A.17}$$

(5) Correlations of Gungor and Winterton [32]:

$$h_{\mathrm{tp}} = Eh_{\mathrm{l}} \tag{A.18}$$

$$E = 1 + 3000Bo^{0.86} + 1.12\left(\frac{x}{1-x}\right)^{0.75}\left(\frac{\rho_{\mathrm{l}}}{\rho_{\mathrm{v}}}\right)^{0.41} \tag{A.19}$$

If the tube is horizontal and the Froude number Fr_{l} is smaller than 0.05, E should be multiplied by the factor

$$E_2 = Fr_{\mathrm{l}}^{\left(0.1-2Fr_{\mathrm{l}}\right)} \tag{A.20}$$

(6) Correlation of Mishra *et al*. [29]:

$$h_{\mathrm{tp,m}} = C_{\mathrm{l}}Bo^{0.15}X_{\mathrm{tt}}^{-0.23} \tag{A.21}$$

(7) Correlations of Sami *et al*. [33]:

$$h_{\mathrm{tp,m}} = 0.015\frac{\lambda_{\mathrm{l}}}{d}\left(\frac{Gd}{\mu_{\mathrm{l}}}\right)^{0.62}A\frac{\lambda_{\mathrm{l}}{}^{0.3}}{100} \tag{A.22}$$

$$A = 1 - 0.79\left(\left|\tilde{y}_1 - \tilde{x}_1\right| + \left|\tilde{y}_2 - \tilde{x}_2\right|\right)^{0.82} \tag{A.23}$$

(8) Correlations of Bivens and Yokozeki [30]:

$$h_{\mathrm{cv}} = F \cdot h_{\mathrm{l}} \cdot R \tag{A.24}$$

$$h_{\mathrm{tp}} = \left(h_{\mathrm{nb}}{}^{2.5} + h_{\mathrm{cv}}{}^{2.5}\right)^{1/2.5} \tag{A.25}$$

$$h_{\mathrm{tp,m}} = h_{\mathrm{tp}} / \left(1 + h_{\mathrm{tp}} \cdot T_{\mathrm{int}} \cdot q\right) \tag{A.26}$$

$$T_{\mathrm{int}} = 0.175\Delta t_{\mathrm{bp}}\left(1 - \exp\left(-q/1.3/10^4/\rho_{\mathrm{l}}/\Delta h_{\mathrm{v}}\right)\right) \tag{A.27}$$

$$F = (0.29 + 1/X_{\mathrm{tt}})^{0.85} \tag{A.28}$$

$$R = 2.15 \quad \text{when} \quad F_{\mathrm{rl}} > 0.25 \tag{A.29}$$

$$R = 2.83 \cdot F_{\mathrm{rl}}^{0.25} \quad \text{when} \quad F_{\mathrm{rl}} \le 0.25 \tag{A.30}$$

(9) Correlation of Shah [13]:

$$N = 0.38F_{\mathrm{rl}}^{-0.3}C_{\mathrm{o}} \quad F_{\mathrm{rl}} < 0.04 \tag{A.31}$$

$$N = C_o \quad F_{\mathrm{rl}} > 0.04 \tag{A.32}$$

$$h_{nb}/h_l = 230Bo^{0.5} \quad N > 1.0, Bo > 0.0003 \tag{A.33}$$

$$h_{nb}/h_l = 1 + 46Bo^{0.5} \quad N > 1.0, Bo < 0.0003 \tag{A.34}$$

$$h_{nb}/h_l = FBo^{0.5}\exp(2.74N^{-0.1}) \qquad 1.0 > N > 0.1 \tag{A.35}$$

$$h_{nb}/h_l = FBo^{0.5}\exp(2.74N^{-0.15}) \qquad N < 0.1 \tag{A.36}$$

$$h_{cv}/h_l = 1.8/N^{0.8} \tag{A.37}$$

$$h_{\mathrm{tp}} = \max\left(h_{\mathrm{cv}}, h_{\mathrm{nb}}\right) \tag{A.38}$$

(10) Grönnerud correlation [39]:

$$\Delta p_{\mathrm{f}} = \Delta p_{\mathrm{l}}\phi_{\mathrm{gd}} \tag{A.39}$$

$$\phi_{\mathrm{gd}} = 1 + \left(\frac{dp}{dz}\right)_{\mathrm{Fr}}\left(\frac{\rho_{\mathrm{l}}/\rho_{\mathrm{v}}}{\left(\mu_{\mathrm{l}}/\mu_{\mathrm{v}}\right)^{0.25}} - 1\right) \tag{A.40}$$

$$\left(\frac{dp}{dz}\right)_{\mathrm{Fr}} = f_{\mathrm{Fr}}\left[x + 4(x^{1.8} - x^{10}f_{\mathrm{Fr}}^{0.5})\right] \tag{A.41}$$

$$f_{Fr} = 1.0, \; F_r > 1.0 \tag{A.42}$$

$$f_{\mathrm{Fr}} = F_{\mathrm{rl}}^{0.3} + 0.0055\left(\ln\frac{1}{F_{\mathrm{rl}}}\right)^2, \; Fr \le 1.0 \tag{A.43}$$

$$F_{\mathrm{rl}} = \frac{G^2}{gd\rho_{\mathrm{l}}^2} \tag{A.44}$$

(11) Correlation of Lockhart–Matinelli [40]:

$$-\left(\frac{dp}{dz}\right)_{\mathrm{f}} = -\left(\frac{dp}{dz}\right)_{\mathrm{l}}\phi_{\mathrm{l}}^2 \tag{A.45}$$

$$\left(-\frac{dp}{dz}\right)_{\mathrm{l}} = 2f_{\mathrm{l}}\frac{G_{\mathrm{l}}^2}{D\rho_{\mathrm{l}}} \tag{A.46}$$

$$\left(-\frac{dp}{dz}\right)_{\mathrm{v}} = 2f_{\mathrm{v}}\frac{G_{\mathrm{v}}^2}{D\,\rho_{\mathrm{v}}} \tag{A.47}$$

$$\phi_{\mathrm{l}}^2 = 1 + C/X + 1/X^2 \tag{A.48}$$

$$X^2 = \frac{(dp/dz)_{\mathrm{l}}}{(dp/dz)_{\mathrm{v}}} \tag{A.49}$$

$$\begin{cases} f_{\mathrm{l}}=0.079\mathrm{Re}_{\mathrm{l}}^{-0.25}, & \mathrm{Re}_{\mathrm{l}}>2000 \\ f_{\mathrm{l}}=16/\mathrm{Re}_{\mathrm{l}}, & \mathrm{Re}_{\mathrm{l}}<2000 \end{cases} \tag{A.50}$$

$$\begin{cases} f_{\mathrm{v}}=0.079\mathrm{Re}_{\mathrm{v}}^{-0.25}, & \mathrm{Re}_{\mathrm{v}}>2000 \\ f_{\mathrm{v}}=16/\mathrm{Re}_{\mathrm{v}}, & \mathrm{Re}_{\mathrm{v}}<2000 \end{cases} \tag{A.51}$$

(12) Müller-Steinhagen and Heck correlation [41]:

$$\left(\frac{dp}{dz}\right)_{\mathrm{Fr}} = C(1-x)^{1/3} + Bx^3 \tag{A.52}$$

$$C = A + 2(B-A)x \tag{A.53}$$

$$A = \left(\frac{dp}{dz}\right)_{\mathrm{l0}} \tag{A.54}$$

$$B = \left(\frac{dp}{dz}\right)_{\mathrm{v0}} \tag{A.55}$$

(13) Friedel correlation [42]:

$$\Delta p_{\mathrm{f}} = \Delta p_{\mathrm{L}}\phi_{\mathrm{f}}^2 \tag{A.56}$$

$$\Delta p_{\mathrm{f}} = 4f_{\mathrm{l}}(L/d)G^2(1/2\rho_{\mathrm{l}}) \tag{A.57}$$

$$f = 0.079\,\mathrm{Re}_{\mathrm{l0}}^{-0.25} \tag{A.58}$$

$$\mathrm{Re}_{\mathrm{l0}} = Gd/\mu_{\mathrm{l}} \tag{A.59}$$

$$\phi = E + \frac{3.24FH}{Fr_{\mathrm{H}}^{0.045}We_{\mathrm{L}}^{0.035}} \tag{A.60}$$

$$E = (1-x)^2 + x^2\frac{\rho_{\mathrm{l}}f_{\mathrm{v}}}{\rho_{\mathrm{v}}f_{\mathrm{l}}} \tag{A.61}$$

$$F = x^{0.78}(1-x)^{0.224} \tag{A.62}$$

$$H = \left(\frac{\rho_{\mathrm{l}}}{\rho_{\mathrm{v}}}\right)^{0.91}\left(\frac{\mu_{\mathrm{v}}}{\mu_{\mathrm{l}}}\right)^{0.19}\left(1-\frac{\mu_{\mathrm{v}}}{\mu_{\mathrm{l}}}\right)^{0.7} \tag{A.63}$$

(14) Correlation of Hwang and Kim [43]:

$$-\left(\frac{dp}{dz}\right)_{\mathrm{f}} = -\left(\frac{dp}{dz}\right)_{\mathrm{l}}\phi_{\mathrm{l}}^2 \tag{A.64}$$

$$\phi_{\mathrm{l}}^2 = 1 + C/X + 1/X^2 \tag{A.65}$$

$$X^2 = \frac{(dp/dz)_{\mathrm{l}}}{(dp/dz)_{\mathrm{v}}} \tag{A.66}$$

$$C = 0.227\,\mathrm{Re}_{\mathrm{l0}}^{0.452}\,X^{-0.32}Bo^{0.41} \tag{A.67}$$

(15) The calculation of parameters in Eqs. (25) and (26)

$$C\left(\eta,\frac{m_1}{m_2},\frac{\varsigma_1}{\varsigma_2},\tilde{x}_1\right) \approx \tilde{x}_1 C\left(\eta,\frac{m_1}{m_2},\frac{\varsigma_1}{\varsigma_2},1\right) + \tilde{x}_2 C\left(\eta,\frac{m_1}{m_2},\frac{\varsigma_1}{\varsigma_2},0\right) \tag{A.68}$$

$$C\left(\eta,\frac{m_1}{m_2},\frac{\tilde{\sigma}_1}{\tilde{\sigma}_2},0\right)\approx 0.84-7.69\left(\eta-0.463\right)-32.3\left(\eta-0.463\right)^2+0.299ln\left(\frac{m_1}{m_2}\right)$$
$$-0.165\left[\ln\left(\frac{m_1}{m_2}\right)\right]^2-0.200\left[\left(\frac{\tilde{\sigma}_1}{\tilde{\sigma}_2}\right)-1\right]-0.78\left[\ln\left(\frac{m_1}{m_2}\right)\right]\left(\eta-0.463\right)$$
$$+0.336\left[\ln\left(\frac{m_1}{m_2}\right)\right]\left[\left(\frac{\varsigma_1}{\varsigma_2}\right)-1\right]-5.33\left(\eta-0.463\right)\left[\left(\frac{\varsigma_1}{\varsigma_2}\right)-1\right] \quad \text{(A.69)}$$

$$C\left(\eta,\frac{m_1}{m_2},\frac{\varsigma_1}{\varsigma_2},1\right)=C\left(\eta,\frac{m_2}{m_1},\frac{\varsigma_1}{\varsigma_2},1\right) \quad \text{(A.70)}$$

The quantity C is introduced to compensate for the neglect by the Enskog theory of the correlation motions in hard sphere fluids. For instance, the collisions of particles in hard sphere fluids are different from those in actual fluids. η_i is the packing fraction of the i-th component, $\eta_i = \pi n_i \sigma_i^3/6$, and $\eta = \eta_1 + \eta_2$. Modification factor A is due to the coupling of translational and rotational degrees of freedom, which is within 0–1 and is equal to 0.55 according to the analysis of Kenneth *et al*. [36].

$$g_{12}\left(\varsigma_{12}\right)=g_{PY}\left(\varsigma_{12}\right)\left[\left(Z_{CS}-1\right)/\left(Z_{PY}-1\right)\right] \quad \text{(A.71)}$$

$$g_{PY}\left(\varsigma_{12}\right)=\left(1+\frac{1}{2}\eta\right)\left(1-\eta\right)^2+\frac{3}{2}\left(\varsigma_1-\varsigma_2\right)\left(\eta_2-\eta_1\right)/\left[\left(1-\eta\right)^2\left(\varsigma_1+\varsigma_2\right)\right] \quad \text{A.72)}$$

$$Z_{cs}=\left(1+\eta+\eta^2-3\eta\left(Y_1+Y_2\eta\right)-Y_3\eta^3\right)/\left(1-\eta\right)^3 \quad \text{(A.73)}$$

$$Z_{PY,v}=\left(1+\eta+\eta^2-3\eta\left(Y_1+Y_2\eta\right)-3Y_3\eta^3\right)/\left(1-\eta\right)^3 \quad \text{(A.74)}$$

The quality of $g_{12}(\varsigma_{12})$ is to reflect that the local density near a particular sphere is greater than the average density, which is related to the compressibility factor and is calculated by the Percus–Yevick pair correlation function between unlike particles in a hard sphere fluid ($g_{PY}(\varsigma_{12})$) in Eq. (A.72). The Carnaban–Starling compressibility factor for a binary mixture (Zcs) and the Percus–Yevick compressibility factor (Z_{PYv}) are calculated by Eqs. (A.73) and (A.74). The quantities Y_i are calculated by Eqs. (A.75–A.78).

$$Y_1=\Delta\times\left(\varsigma_1+\varsigma_2\right)/\left(\varsigma_1\varsigma_2\right)^{1/2} \quad \text{(A.75)}$$

$$Y_2=\Delta\times\left(\varsigma_1\varsigma_2\right)^{1/2}\left(\eta_1/\varsigma_1+\eta_2/\varsigma_2\right)/\eta \quad \text{(A.76)}$$

$$Y_3=\left[\left(\eta_1/\eta\right)^{2/3}\tilde{x}_1^{1/3}+\left(\eta_2/\eta\right)^{2/3}\tilde{x}_2^{1/3}\right]^3 \quad \text{(A.77)}$$

$$\Delta=\left(\eta_1\eta_2\right)^{1/2}\left[\left(\varsigma_1-\varsigma_2\right)^2/\varsigma_1\varsigma_2\right]\left(\tilde{x}_1\tilde{x}_2\right)^{1/2}/\eta \quad \text{(A.78)}$$

REFERENCES

[1] M. Spatz, B. Minor, HFO1234yf low GWP refrigerant: A global sustainable solution for mobile air conditioning, SAE Alternate Refrigerant Systems Symposium, Scottsdale, AZ, 2008.

[2] M.X. Li, C. Dang, E. Hihara, Flow boiling heat transfer of HFO1234yf and HFC32 refrigerant mixtures in a smooth horizontal tube, Part I: Experimental investigation, International Journal of Heat and Mass Transfer 55 (2012) 3437-3446.

[3] J.C. Chen, Correlation for boiling heat transfer to saturated fluids in convective flow, Industry Chemical Engineering Process Design and Development 5(3) (1966) 322-339.

[4] H.K. Forster, N. Zuber, Dynamics of vapour bubbles and boiling heat transfer, Chemical Engineering Progress 1(4) (1955) 531-535.

[5] J.C. Chen, K. Tuzla, Contributions of convection and boiling to convective flow boiling, in: J.C. Chen (Ed.), Convective Flow Boiling, Taylor & Francis, Washington, 1995, pp. 181-186.
[6] K.E. Gunger, R.H.S. Winterton, A general correlation for flow boiling in tubes and annuli, International Journal of Heat and Mass Transfer 29(3) (1986) 351-358.
[7] M.G. Cooper, Heat flow rates in saturated nucleate pool boiling—a wide-ranging examination using reduced properties, Advances in Heat Transfer 16 (1984) 157-239.
[8] S. Yoshida, H. Mori, H. Hong, T. Matsunaga, Prediction of heat transfer coefficient for refrigerants flowing in horizontal evaporator tubes, Transcripts of the JAR 11(1) (1994) 67-78.
[9] L. Zhang, E. Hihara, T. Saito, J. Oh, Boiling heat transfer of a ternary refrigerant mixture inside horizontal smooth tube, International Journal of Mass Transfer 40(9) (1997) 2009-2017.
[10] K. Stephan, M. Abdelsalam, Heat transfer correlation for natural convection boiling, International Journal of Heat and Mass Transfer 23 (1980) 73-87.
[11] S.S. Kutateladze, Boiling heat transfer, International Journal of Heat and Mass Transfer 4 (1961) 3-45.
[12] D. Steiner, J. Taborek, Flow boiling heat transfer in vertical tubes correlated by an asymptotic model, Heat Transfer Engineering 13(2) (1992) 43-69.
[13] M.M. Shah, A new correlation for heat transfer during boiling flow through pipes, ASHRAE Transcripts 82(2) (1976) 66-86.
[14] S.G. Kandlikar, A general correlation for two-phase flow boiling heat transfer coefficients inside horizontal and vertical tubes, Journal of Heat Transfer 112 (1990) 219-228.
[15] V. Gnielinski, New equations for heat and mass transfer in turbulent pipe and channel flow, International Chemical Engineering 16 (1976) 359-368.
[16] S. Saitoh, C. Dang, Y. Nakamura, E. Hihara, Boiling heat transfer of HFO1234yf flowing in smooth small-diameter horizontal tube, International Journal of Refrigeration 34(8) (2011) 1846-1853.
[17] S. Saitoh, H. Daiguji, E. Hihara, Correlation for boiling heat transfer of R-134a in horizontal tubes including effect of tube diameter, International Journal of Heat and Mass Transfer 50 (2007) 5215-5225.
[18] J.Y. Shin, M.S. Kim, S.T. Ro, Experimental study on forced convective boiling heat transfer of pure refrigerants and refrigerant mixtures in a horizontal tube, International Journal of Refrigeration, 20(4) (1997) 267-275.
[19] K.E. Gungor, R.H.S. Winterton, Simplified general correlation for saturated flow boiling and comparisons of correlations, Chemical Engineering Research and Design 65 (1987) 148-156.
[20] T. Kamiaka, C. Dang, E. Hihara, Vapor-liquid equilibrium measurements for binary mixtures of R1234yf with R32, R125, and R134a, International Journal of Refrigeration 36(3) (2013) 965-971.
[21] L.E. Scriven, On the dynamics of phase growth, Chemical Engineering Science 10 (1959) 1-13.
[22] S.J.D. Van Stralen, M.S. Sohal, R. Cole, W.M. Sluyter, Bubble growth rates in pure and binary systems: Combined effect of relaxation and evaporation microlayers, International Journal of Heat and Mass Transfer 18 (1975) 453-467.
[23] W.R. Van Wijk, A.S. Vos, S.J.D. Stralen, Heat transfer to boiling binary liquid mixtures Chemical Engineering Science 5 (1956) 68-80.
[24] K. Stephan, M. Körner, Berechnung des Wärmeübergangs verdampfender binärer Flüssigkeitsgemische, Chemie Ingenieur Technik 41(7) (1969) 409-417 (in German).
[25] W.F. Calus, D. J. Leonidopulos, Pool boiling—Binary liquid mixtures, International Journal of Heat and Mass Transfer 17 (1974) 249-256.
[26] J.R. Thome, R.A.W. Shock, Boiling of multicomponent liquid mixtures, Advances in Heat Transfer 16 (1986) 60-157.
[27] D.L. Bennet, J.C. Chen, Forced convective boiling in vertical tubes for saturated pure components and binary mixtures, AIChE Journal 26(3) (1980) 454-461.
[28] D.S. Jung, M. Mclinden, R. Radmeracher, D. Didion, A study of flow boiling heat transfer with refrigerant mixtures, International Journal of Heat and Mass TransfeHFC32(9) (1989) 1751-1764.
[29] M.P. Mishra, H.K. Varma, C.P. Sharma, Heat transfer coefficients in forced convection evaporation of refrigerant mixtures, Letters in Heat Mass Transfer 8 (1981) 127-136.
[30] D.B. Bivens, A. Yokozeki, Heat transfer coefficients and transport properties for alternative refrigerants, in: Proceeding of International Refrigeration Conference at Purdue, West Lafayette, IN, 1994, pp. 229-304.

[31] J.P. Wattelet, J.C. Chato, A.L. Souza, B.R. Christofferson, Initial evaporative comparison of R-22 with alternative refrigerants R134a and HFC32/R125, Air Conditioning and Refrigeration Center Report TR-39, University of Illinois, 1993.
[32] E.W. Lemmon, M.L. Hube, M.O. Mclinden, Physical and chemical properties division, REFPROP 8.0, NIST Standard Reference Database 23, Version 8.0.
[33] S.M. Sami, J. Schnotale, J.G. Smale, Prediction of the heat transfer characteristics of R22/R152a/R114 and R22/R152a/R124, ASHRAE Transactions 98(2) (1992) 51-58.
[34] J.Y. Shin, M.S. Kim, S.T. Ro, Correlation of evaporative heat transfer coefficients for refrigerant mixtures, Proceedings of the International Refrigeration Conference at Purdue, West Lafayette, IN, 1996, pp. 151-156.
[35] J.W. Palen, W. Small, A new way to design kettle and internal reboilers, Hydrocarbon Processing 43(11) (1964) 199-208.
[36] J.C. Kenneth, H.C. Andersen, R. Pecora, Light scattering measurement and theoretical interpretation of mutual coefficients in binary liquid mixtures, Chemical Physics 11 (1975) 451-473.
[37] J.R. Thome, Engineering data book III, Wolverine Tube, Inc. 2004, p.13-4
[38] D. Steiner, VDI-Wärmeatlas (VDI Heat Atlas), Verein Deutscher Ingenieure, DI-Gesellschaft Verfahrenstechnik und Chemieingenieurwesen (GCV), Düsseldorf, Chapter Hbb, 1993.
[39] R. Grönnerud, Investigation in liquid holdup, flow resistance and heat transfer in circular type evaporators, Part IV: two-phase resistance in boiling refrigerants, bulletin de l'Inst. Du Froid, Annexe 1972-1.
[40] S.M. Ghiaasiaan, Two-phase flow, boiling, and condensation in conventional and miniature systems, Cambridge University press, 2008, p. 261.
[41] H. Müller-Steinhagen, K. Heck, A simple friction pressure drop correlation for two-phase flow pipes, Chem. Eng. Process. 20 (1986) 297-308.
[42] L. Friedel, Improved friction pressure drop correlations for horizontal and vertical two-phase pipe flow, in: European Two-Phase Flow Group Meeting, Ispra, Italy, 1979, paper E2.
[43] Y.W. Hwang, M.S. Kim, The pressure drop in microtubes and the correlation development, International Journal of Heat and Mass Transfer 49 (2006) 1804-1812.

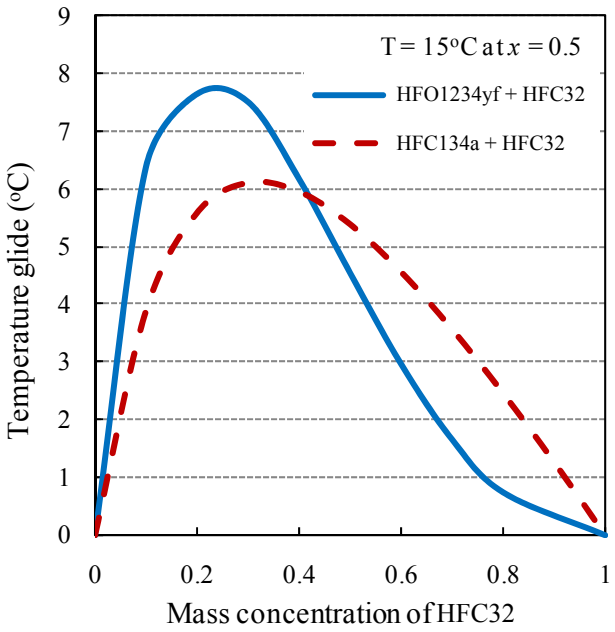

Figure 1 Temperature glides of HFC134a + HFC32 and HFO1234yf + HFC32 mixtures.

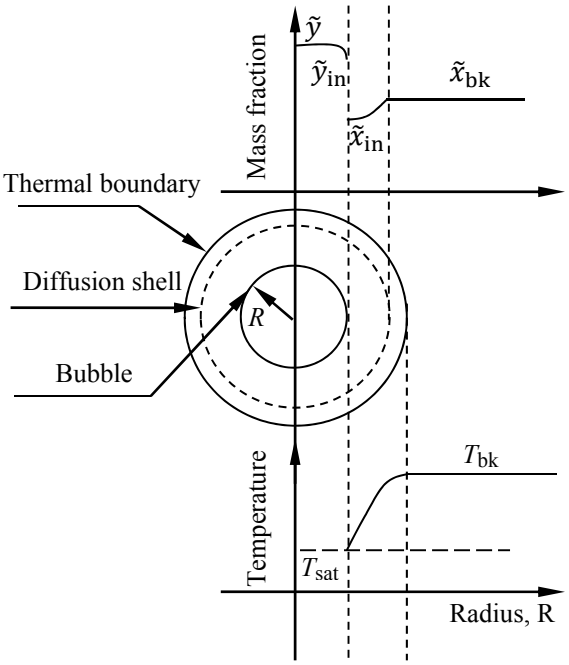

Figure 2 Composition and temperature distribution around bubble in mixture.

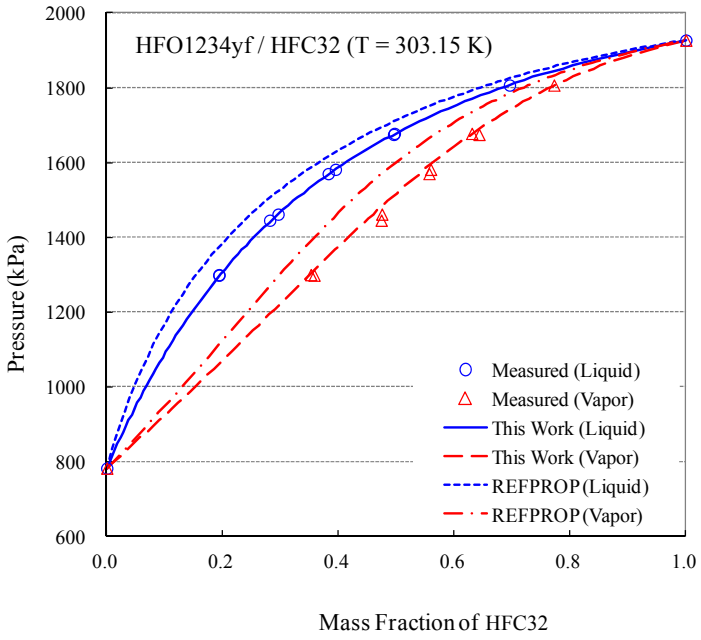

Figure 3 Comparison of the Peng–Robinson model from Kamiaka *et al*. [20] and REFPROP [32].

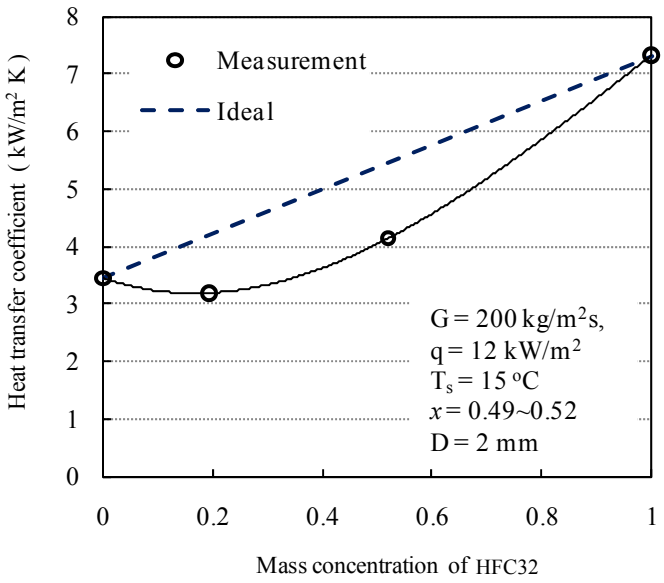

Figure 4 Heat transfer coefficient of mixture at different concentrations.

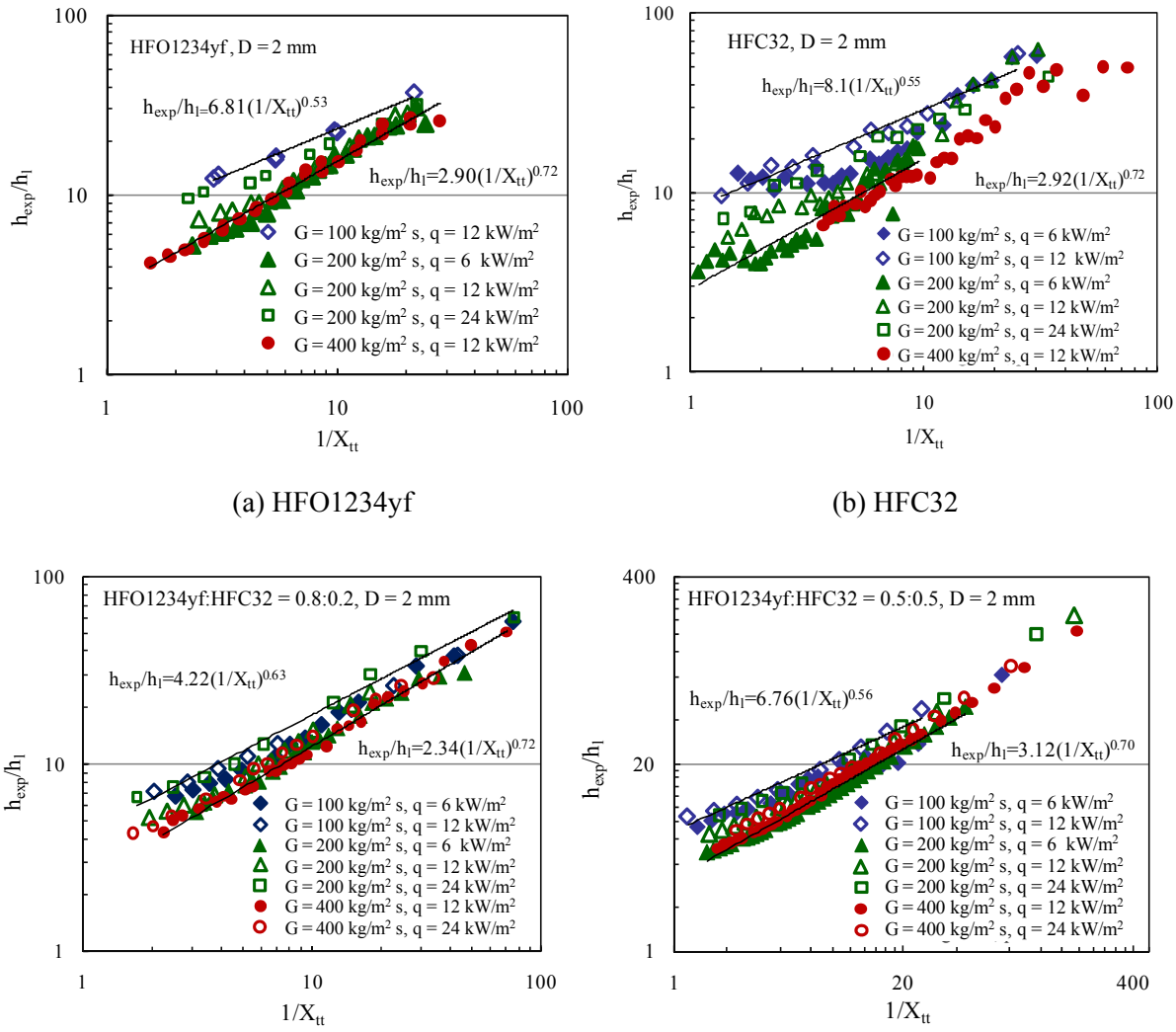

(a) HFO1234yf

(b) HFC32

(c) HFO1234yf:HFC32 = 0.8:0.2

(d) HFO1234yf:HFC32 = 0.5:0.5

Figure 5 Boiling heat transfer coefficients as function of the Lockhart–Martinelli parameter.

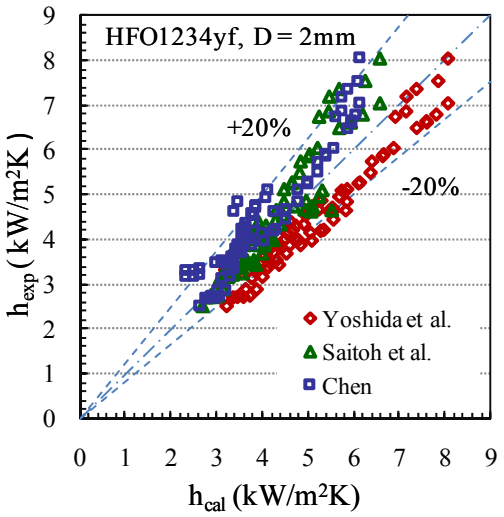

(a) HFO1234yf

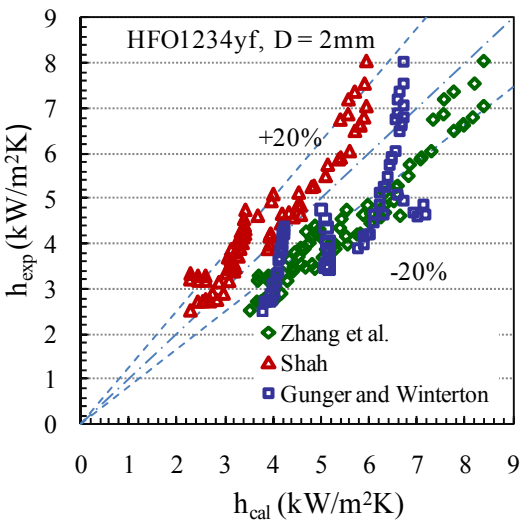

(b) HFO1234yf

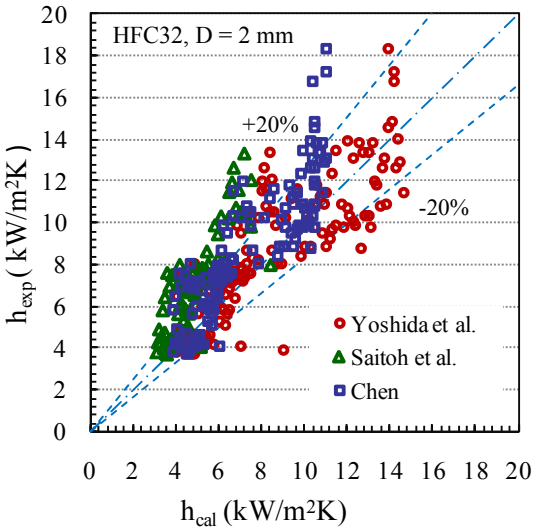

(c) HFC32

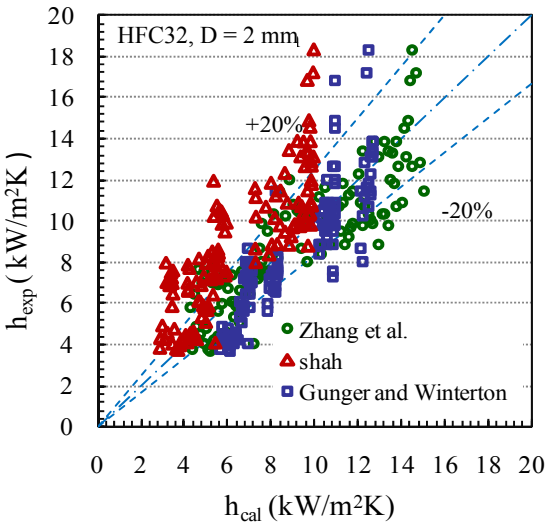

(d) HFC32

Figure 6 Experimental heat transfer coefficients for HFO1234yf and HFC32 versus heat transfer coefficients predicted using available correlations.

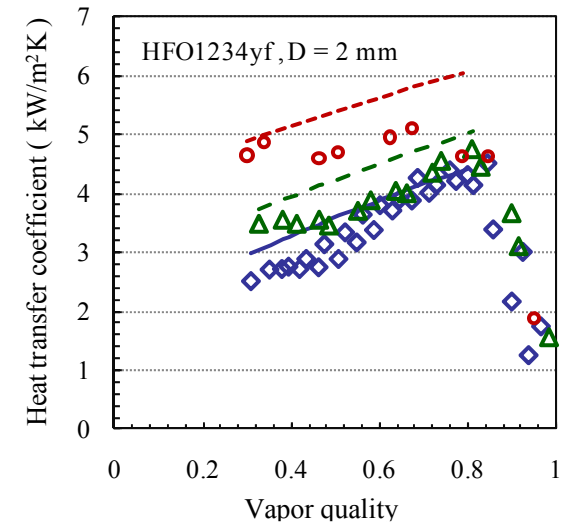

(a) HFO1234yf, G = 200 kg/m^{2}s

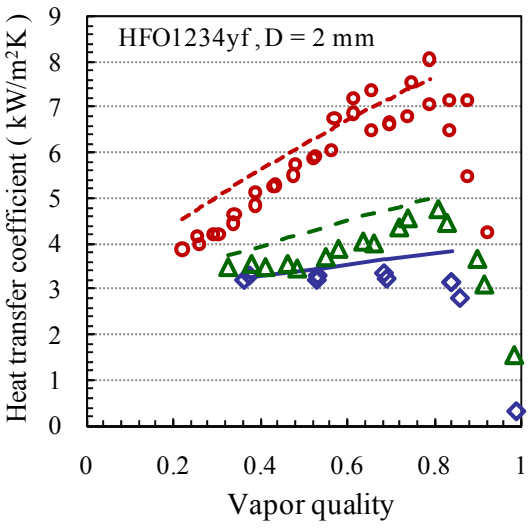

(b) HFO1234yf, q = 12 kW/m^2

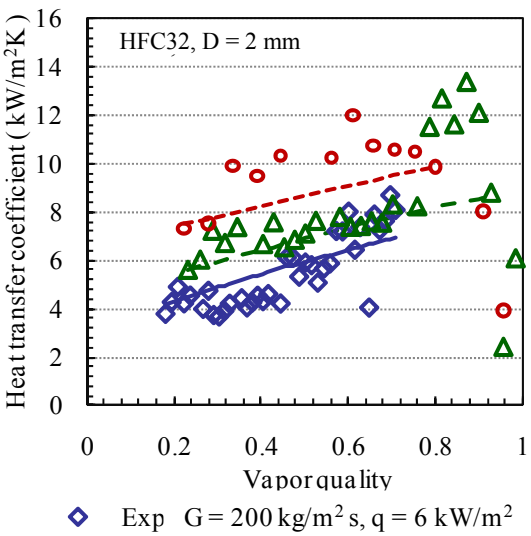

(c) HFC32, G = 200 kg/m^{2}s

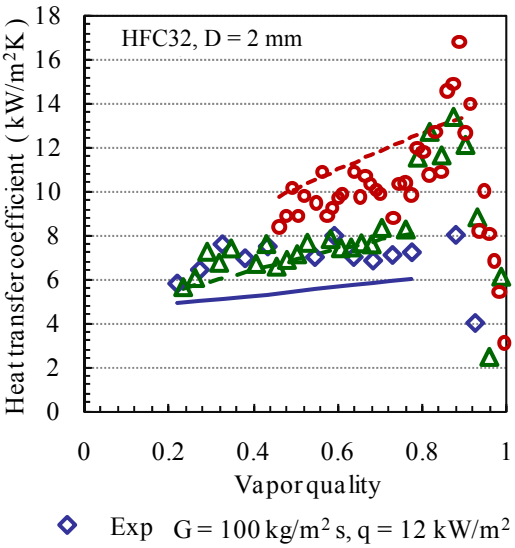

(d) HFC32, q = 12 kW/m^2

Figure 7 Heat transfer coefficients as function of vapor quality for pure HFO1234yf and pure HFC32: comparison of experimental results with predictions by the proposed correlation.

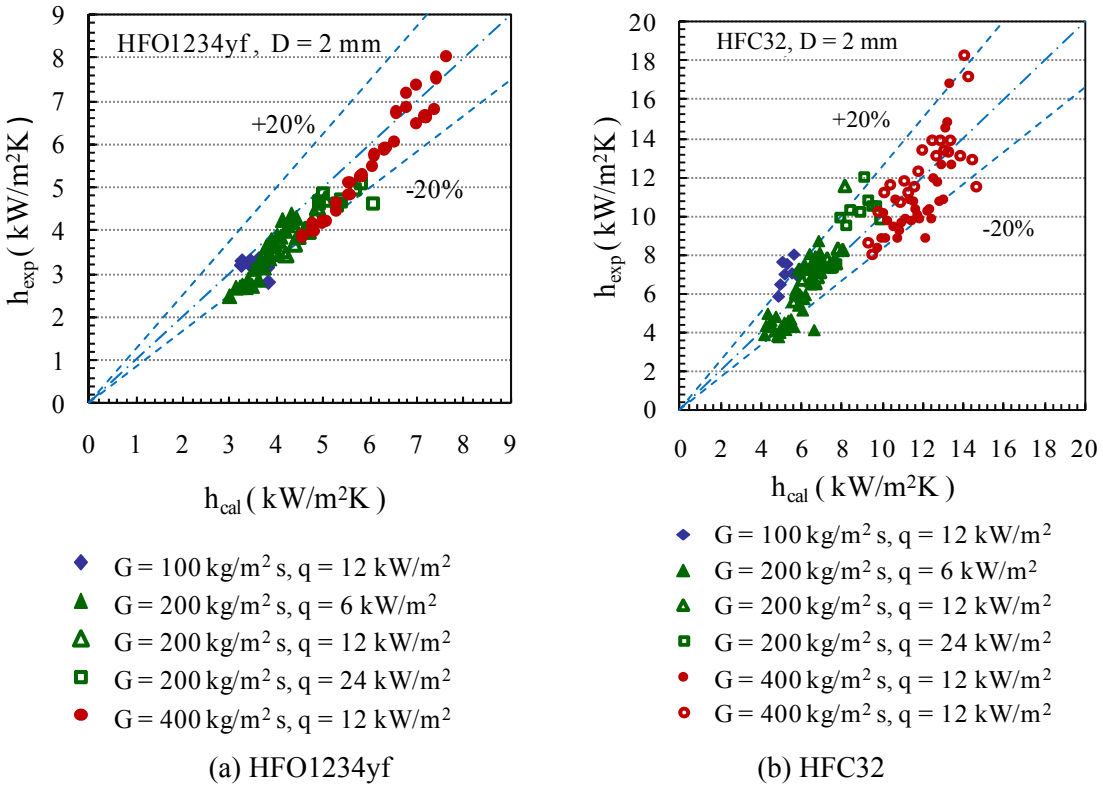

(a) HFO1234yf (b) HFC32

Figure 8 Experimental heat transfer coefficients for HFO1234yf and HFC32 versus heat transfer coefficients predicted using the proposed correlation.

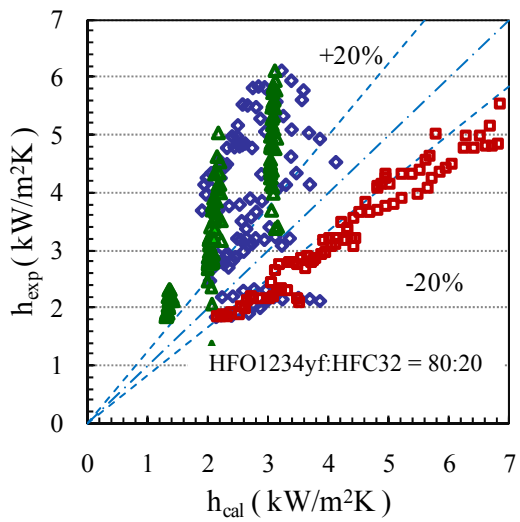

(a) HFO1234yf:HFC32 = 80:20

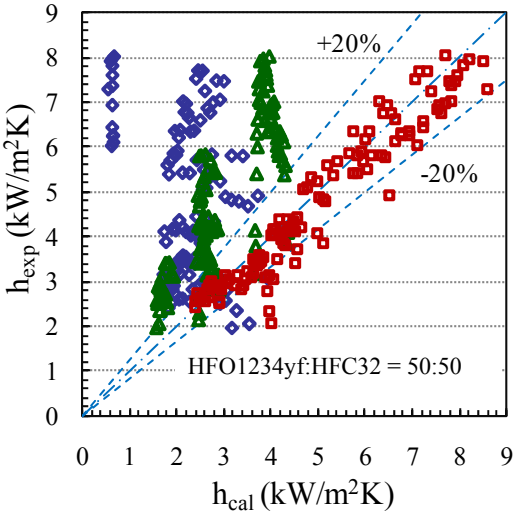

(b) HFO1234yf:HFC32 = 50:50

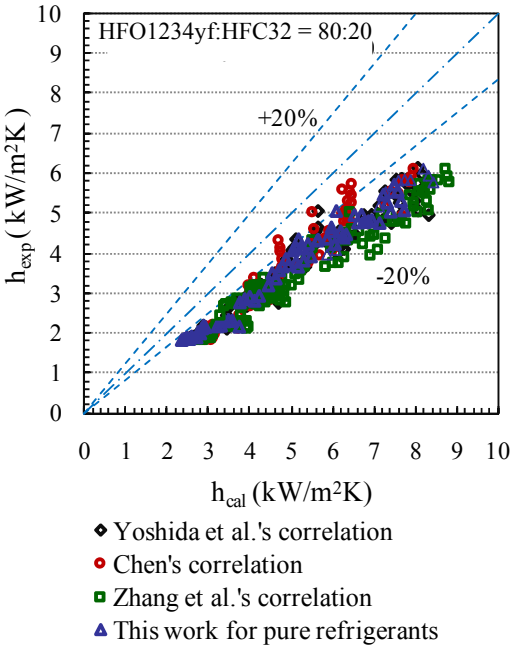

(c) HFO1234yf:HFC32 = 80:20

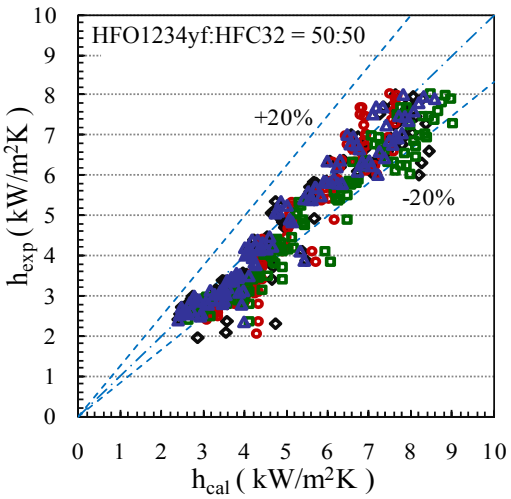

(d) HFO1234yf:HFC32 = 50:50

Figure 9 Results predicted for HFO1234yf + HFC32 mixtures by seven correlations.

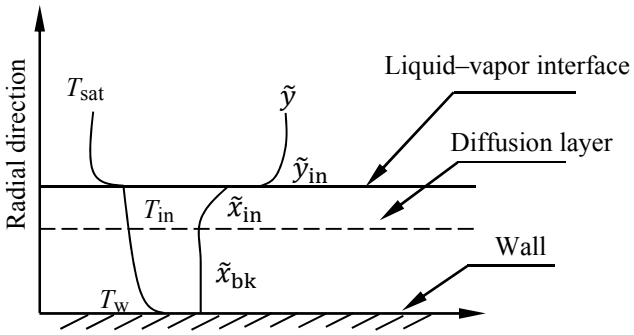

Figure 10 Distribution of temperatures and composition of the mixture in radial direction

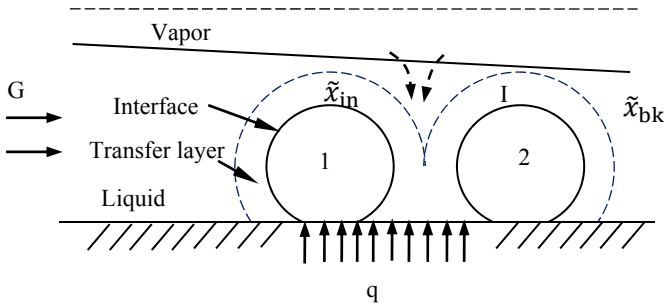

(a) High *Bo*

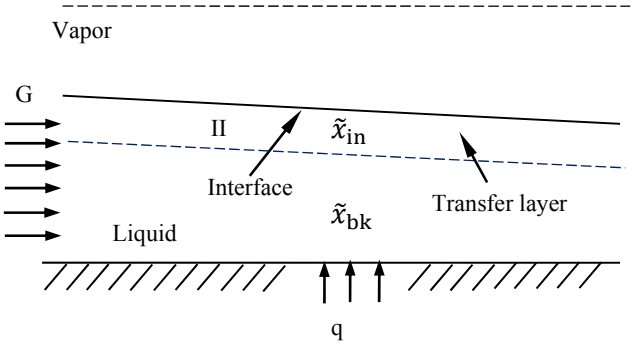

(b) Low *Bo*

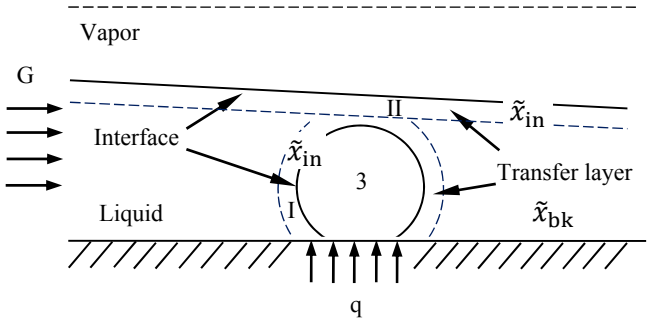

(c) Moderate *Bo*

Figure 11 Flow boiling situation of mixtures at various *Bo*.

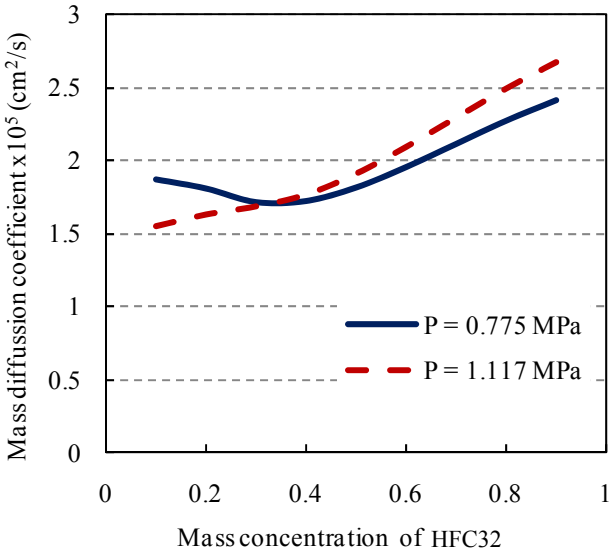

Figure 12 Mass diffusion coefficients of mixtures.

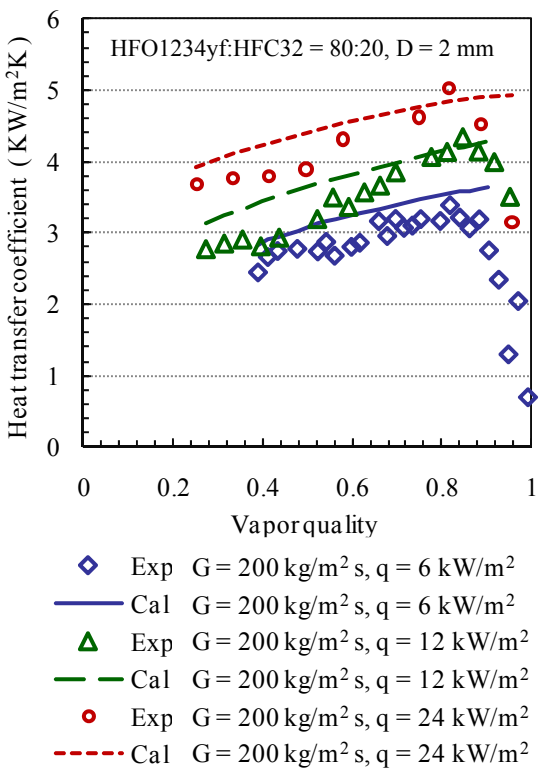

(a) HFO1234yf:HFC32 = 80:20, G = 200 kg/m^{2}s

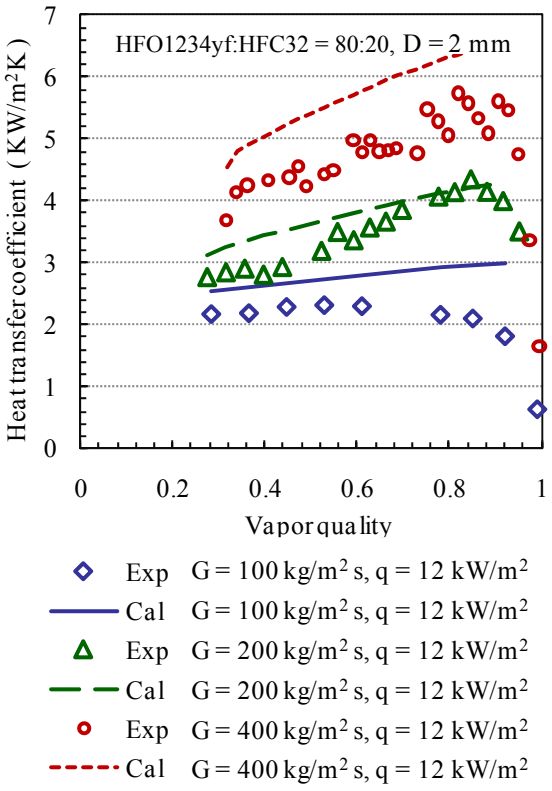

(b) HFO1234yf:HFC32 = 80:20, q = 12 kW/m^2

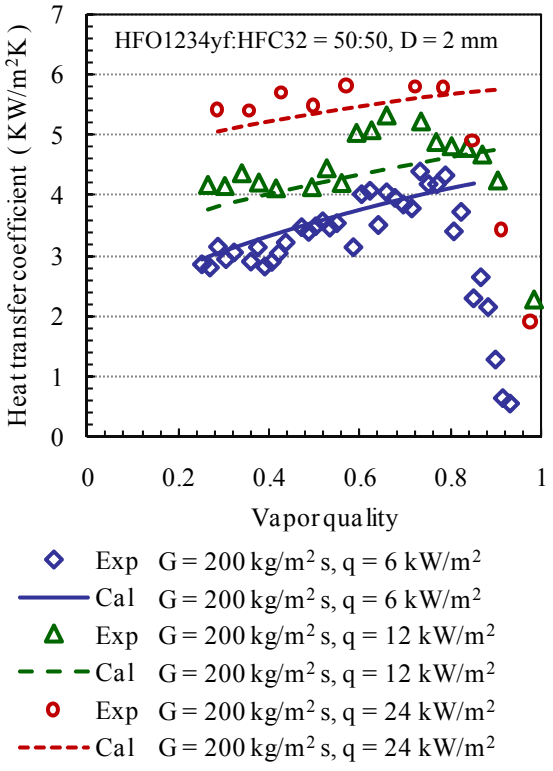

(c) HFO1234yf:HFC32 = 50:50, G = 200 kg/m^{2}s

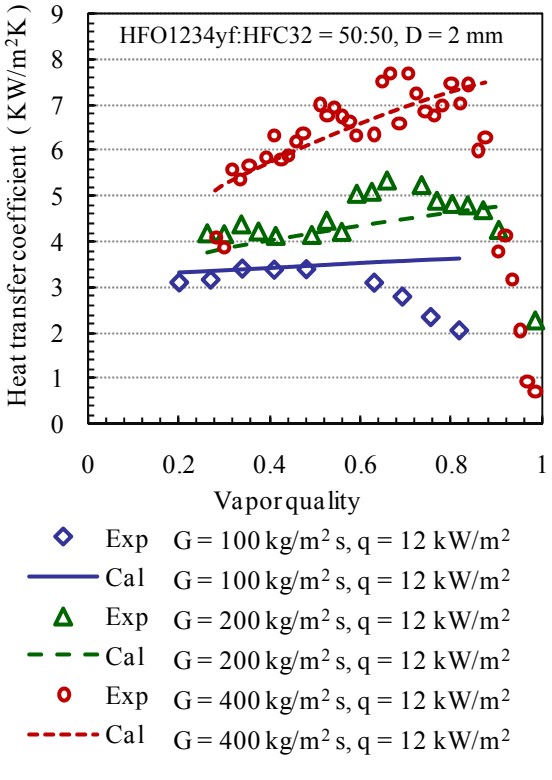

(d) HFO1234yf:HFC32 = 50:50, q = 12 kW/m^2

Figure 13 Comparison of experimental results with predictions by the proposed correlation.

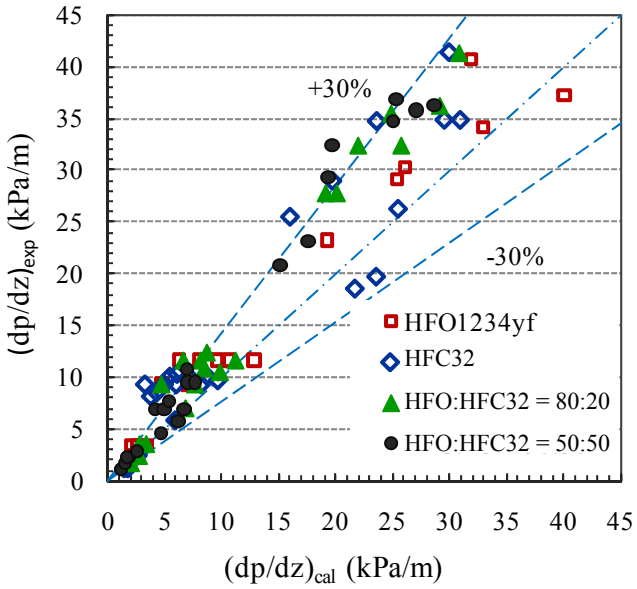

Figure 14 Comparison of experimental pressure drops with predicted values by using Müller–Steinhagen and Heck [41] model.

Table 1 Experimental conditions

Refrigerant	HFO1234yf	HFC32	HFO1234yf + HFC32	HFO1234yf + HFC32
Concentration wt%	100	100	80:20	50:50
Quality	0.2–1.0			
Heat flux (kW/m^2)	6, 12, 24			
Mass flux (kg/m^{2}s)	100, 200, 400			
Data number	75	164	99	138

Table 2 Deviations in predictions of heat transfer coefficients for pure HFO1234yf

Mass flux (kg/m^2s), Heat flux (kW/m^2)	Chen [3]	Yoshida *et al*. [8]	Zhang *et al*. [9]	Shah [13]	Saitoh *et al*. [17]	Gunger and Winterton [19]	This work
100, 12	*0.235*	0.045	0.188	*0.252*	0.046	*0.377*	0.061
200, 6	0.086	0.195	*0.277*	0.112	0.065	*0.223*	0.114
200, 12	0.099	0.175	*0.301*	0.164	0.046	*0.331*	0.130
200, 24	0.198	0.157	*0.320*	0.118	0.080	*0.432*	0.138
400, 12	0.092	0.142	*0.224*	0.114	0.112	0.186	0.098

Note: Italicized numbers indicate that the deviation is greater than 0.2.

Table 3 Deviations in predictions of heat transfer coefficients for pure HFC32

Mass flux (kg/m^2s), Heat flux (kW/m^2)	Chen [3]	Yoshida *et al*. [8]	Zhang *et al*. [9]	Shah [13]	Saitoh *et al*. [17]	Gunger and Winterton [19]	This work
100, 6	*0.312*	*0.276*	*0.225*	*0.483*	*0.424*	*0.254*	*0.243*
100, 12	*0.367*	*0.341*	*0.278*	*0.525*	*0.426*	0.060	*0.220*
200, 6	0.146	0.154	0.183	*0.286*	*0.211*	*0.293*	0.153
200, 12	0.192	0.147	0.066	*0.344*	*0.321*	0.149	0.069
200, 24	*0.303*	*0.213*	0.141	*0.406*	*0.319*	0.130	0.114
400, 12	0.087	0.168	0.195	0.197	0.148	0.112	0.135
400, 24	0.201	0.103	0.082	*0.301*	*0.292*	0.134	0.087

Note: Italicized numbers indicate that the deviation is greater than 0.2.

Table 4 Deviations in predictions of heat transfer coefficients for HFO1234yf + HFC32 (80/20 by mass%)

Mass flux (kg/m^2s), Heat flux (kW/m^2)	Chen [3]	Yoshida *et al*. [8]	Zhang *et al*. [9]	Mishra *et al*. [29]	Bivens and Yokozeki [30]	Sami *et al*. [33]	This work
100, 6	*0.533*	*0.369*	*0.507*	*0.322*	*0.248*	*0.329*	*0.345*
100, 12	*0.686*	*0.507*	*0.691*	*0.226*	*0.462*	*0.379*	*0.540*
200, 6	*0.356*	*0.397*	*0.477*	0.147	*0.290*	*0.307*	*0.329*
200, 12	*0.345*	*0.344*	*0.489*	*0.226*	*0.235*	*0.375*	*0.323*
200, 24	*0.300*	*0.314*	*0.506*	*0.301*	*0.277*	*0.485*	*0.337*
400, 12	*0.275*	*0.430*	*0.516*	*0.450*	*0.337*	*0.359*	*0.382*
400, 24	*0.374*	*0.390*	*0.537*	*0.265*	*0.334*	*0.380*	*0.386*

Note: Italicized numbers indicate that the deviation is greater than 0.2.

Table 5 Deviations in predictions of heat transfer coefficients for HFO1234yf + HFC32 (50/50 by mass%)

Mass flux (kg/m^2s), Heat flux (kW/m^2)	Chen [3]	Yoshida *et al.* [8]	Zhang *et al.* [9]	Mishra *et al.* [29]	Bivens and Yokozeki [30]	Sami *et al.* [33]	This work
100, 6	*0.218*	0.052	0.087	0.167	0.060	*0.371*	0.057
100, 12	*0.394*	0.155	*0.299*	*0.269*	*0.238*	*0.416*	*0.222*
200, 6	0.208	0.137	*0.236*	*0.361*	0.092	0.208	0.098
200, 12	0.101	0.056	0.115	*0.421*	0.067	*0.417*	0.054
200, 24	0.169	0.036	0.164	*0.459*	0.110	*0.496*	0.042
400, 12	0.078	0.099	0.138	*0.619*	0.088	*0.345*	0.072
400, 24	0.083	0.094	0.189	*0.607*	0.102	*0.410*	0.089

Note: Italicized numbers indicate that the deviation is greater than 0.2.

Table 6 Deviations in predictions of heat transfer coefficients for HFO1234yf + HFC32 (80/20 by mass%) using suppression factors for mixtures

Mass flux (kg/m^{2}s), Heat flux (kW/m^2)	Chen [3]	Yoshida *et al*. [8]	Zhang *et al*. [9]	This work
100, 6	0.156	0.145	0.192	0.080
100, 12	*0.264*	*0.227*	*0.357*	0.209
200, 6	0.095	0.195	0.192	0.113
200, 12	0.178	0.143	*0.249*	0.093
200, 24	0.158	0.100	*0.220*	0.068
400, 12	0.107	*0.246*	*0.321*	0.203
400, 24	0.160	0.194	*0.312*	0.193

Note 1: The factors S_{mix} and F_{mix} are applied to all the correlations.
Note 2: Italicized numbers indicate that the deviation is greater than 0.2.

Table 7 Deviations in predictions of heat transfer coefficients for HFO1234yf + HFC32 (50/50 by mass%) using suppression factors for mixtures

Mass flux (kg/m^{2}s), Heat flux (kW/m^2)	Chen [3]	Yoshida *et al*. [8]	Zhang *et al*. [9]	This work
100, 6	0.123	0.105	0.086	0.084
100, 12	*0.299*	0.091	0.172	0.146
200, 6	0.130	0.066	0.124	0.067
200, 12	0.071	0.084	0.057	0.070
200, 24	0.091	0.085	0.051	0.063
400, 12	0.068	0.076	0.099	0.072
400, 24	0.071	0.061	0.151	0.053

Note 1: The factors S_{mix} and F_{mix} are applied to all the correlations.
Note 2: Italicized numbers indicate that the deviation is greater than 0.2.

Table 8 Deviations in predictions of pressure drop for pure refrigerants and mixtures

Models	HFO	HFC32	HFO:HFC32 = 80:20	HFO:HFC32 = 50:50
Grönnerud [39]	*0.360*	*0.388*	0.302	0.249
Lockhart–Matinelli [40]	0.238	*0.377*	0.267	0.259
Müller-Steinhagen and Heck [41]	0.203	0.268	0.221	0.220
Friedel [42]	*0.632*	*0.614*	*0.606*	*0.660*
Hwang and Kim [43]	*0.572*	*0.613*	*0.623*	*0.650*

Note 2: Italicized numbers indicate that the deviation is greater than.0.3